ESTIMATING RAINFALL INTERCEPTION LOSS USING SENTINEL-2 IN THE VELUWE AREA, THE NETHERLANDS

JOSEPH HAHIRWABASENGA
February, 2019

SUPERVISORS:

Dr.ir. Christiaan Van der tol
Dr.ir. Chris Mannaerts

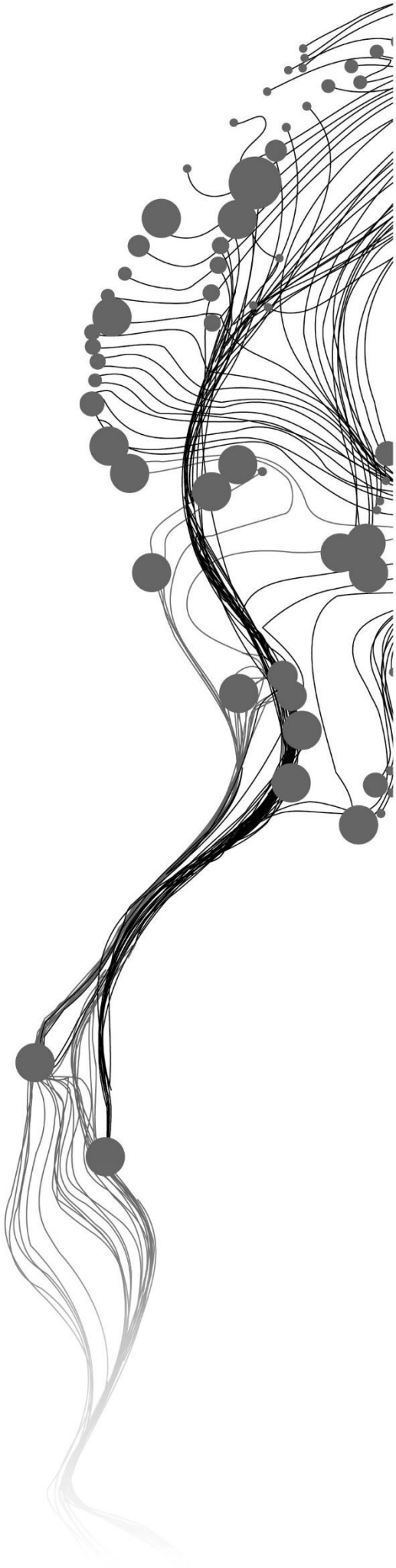

ESTIMATING RAINFALL INTERCEPTION LOSS USING SENTINEL-2 IN THE VELUWE AREA, THE NETHERLANDS

JOSEPH HAHIRWABASENGA
Enschede, The Netherlands, February, 2019

Thesis submitted to the Faculty of Geo-Information Science and Earth Observation of the University of Twente in partial fulfillment of the requirements for the degree of Master of Science in Geo-information Science and Earth Observation.
Specialization: Water Resources and Environmental Management

SUPERVISORS:

Dr.ir. Christiaan Van der tol
Dr.ir. Chris Mannaerts

THESIS ASSESSMENT BOARD:

Chairman: Dr. M.W. Lubczynski, WRS, ITC, Enschede
External Examiner: Dr. Sajid Pareeth, IHE Delft Institute for water Eduction

ABSTRACT

The process of rainfall interception plays a big role in the hydrological cycle. Interception loss from forested areas is significant and can have a serious impact on water balance. The amount of rainfall which is intercepted basically depends on vegetation properties, such as canopy structure, leaf phenology, and density. Therefore, the description of the spatial and temporal variation of vegetation is very important in the estimation of interception loss. This research is aimed at quantification of rainfall interception loss of different land cover classes on the large area using remote sensing method. The study area is the Veluwe forested area central part of the Netherlands in the western part of Gelderland province. In this study, leaf area index (LAI) and fractional vegetation cover (FVC) maps of the study area were derived from Sentinel-2 time series images of June to December 2016 (excluding November, because all the images of this month were affected by clouds). Five land cover classes (broad-leaved forest, coniferous forest, mixed forest, pastures, and natural grassland) were selected to assess the spatial and temporal variation of leaf area index and fractional vegetation cover. The mean LAI values range from 0.3 to 2.8. The mean FVC values range from 11% to 67%.

The monthly canopy storage capacity of each land cover was estimated. Therefore, knowing the canopy storage capacity and other vegetation properties of different land cover classes, different interception losses can be estimated using remote sensing method. In the present study, to estimate rainfall interception loss per land cover class, remote sensing (RS) Gash model was used, and event-based rainfall analysis was carried out in each month. The rainfall interception was estimated based on wet vegetation canopy (gross rainfall greater than 0.5 mm). The mean interception loss per landcover class in the whole season (June to December 2016) for broadleaf forest (BLF), coniferous forest (CF), mixed forest (MF), pastures (PS) and grassland (NGL) are 28.7% , 27.8%, 27.6% , 20.4% , and 16.2% of total rainfall respectively . Broad-leaved forest has high interception loss due to their maximum leaf area index which leads to high canopy storage capacity. In general, forests have large interception loss than other land cover types such as pastures and grassland.

Temporal variability of interception loss in the whole season the mean monthly interception loss is 25.3%, 31.6%, 28.3%, 32.1%, 15.1%, and 12.3% of gross rainfall in June, July, August, September, October and December 2016 respectively. The high interception found in the months of summer season when the vegetations are at their peak productivity and the low interception found in December (winter season) when the most vegetations shade off their leaves, this reduction in leaf amounts cause decrease in intercepted rainfall, there is significant relationship between interception loss and leaf area index. From sensitivity analysis of five main parameters to the interception loss simulated by remote sensing Gash model shows that the fractional vegetation cover is the most sensitive parameter to the simulated interception loss. As the fractional vegetation cover increases the interception loss increases rapidly.

The comparison between measured and estimated interception loss at the coniferous plot. From the previous study by Cisneros et al. (2018) reported the measured interception loss of 39% of gross rainfall whereas the estimated interception loss of the present study is 30% of gross rainfall. The model of the present study underestimates the interception loss by 9% of gross rainfall. Therefore it is very important to measure and monitor LAI and Smax of different land cover classes in order to quantify rainfall interception losses.

Keywords: Remote sensing, rainfall interception, Sentinel-2, Gash, Forest, and the Netherlands

ACKNOWLEDGEMENT

Let me first gratitude to my first supervisor Dr. Christiaan van der Tol for his generous support throughout the whole research. His critical comments and guidance were very fruitful for successful of my research; without him, I couldn't make it.
I extend gratitude to my second supervisor Dr. Chris Mannaerts for his suggestions and comments, from the first day of my research proposal, especially during data pre-processing.

My sincere thanks also, to all the members of the water resources department including the professors and staff for providing me the knowledge and skills to carry out this M.Sc. Research.
Finally, I cannot forget to appreciate and thanks to the Netherlands Fellowship Program (NFP) for funding me to study this M.Sc. Degree.

TABLE OF CONTENTS

LIST OF FIGURES

LIST OF TABLES

LIST OF ABBREVIATIONS

CLC	Corine Land Cover
ESA	European Space Agency
BLF	Broad-Leaf Forest
CF	Coniferous Forest
MF	Mixed Forest
PS	Pastures
NGL	Natural Grass Land
LAI	Leaf Area Index
FVC	Fractional Vegetation Cover
SMAX	Canopy Storage Capacity
UTM	Universal Transverse Mercator
WGS	World Geodetic System
KNMI	Royal Netherlands Meteorological Institute
SNAP	Sentinel application platform
GIS	Geographic Information System
GMES	Global Monitoring for Environment and Security
SWIR	Short Wavelength Infrared
MSI	Multispectral Instrument
BOA	Bottom Of Atmosphere
PG	Gross rainfall
ITC	International Institute for Geo-information Science and Earth observation
RS	Remote Sensing
MODIS	Moderate Resolution Imaging Spectral-Radiometer
NAP	" Normaal Amsterdams Peil"
SAFE	Standard Archive Format for Europe
EEA	European Environmental Agency
MMU	Minimum Mapping Unit

1. INTRODUCTION

1.1. Background

Rainfall intercepted by the vegetation canopies and its evaporation plays a crucial role in water balance. For long time vegetation like forests have been recognized as a vital source of clean drinking water, the high percentage of water for domestic and agricultural use served by forested areas (Calder, Hofer, Vermont, & Warren, 2007). Forests improve the water cycle by reducing runoff where rainfall intercepted by vegetation canopies slows the forces of raindrops reaching the ground. Furthermore, forests planted along lakes and streams minimize water pollution. For instance, pollutants like fertilizers and pesticides are reduced before entering the waterways (Ekhuemelo, 2016). However, forests enhance evaporation where a massive amount of rainwater evaporates back to the atmosphere through interception loss, and it has been proven that interception loss is always high in forested areas compared to other land cover types (Cosandey et al., 2003).

Therefore, estimation of interception loss is crucial for water balance in surface hydrology, particularly in the forested area, it can be used to predict the practical use of water and its distribution. The interception models are useful in the determination of interception. The important part during the quantification of intercepted water by vegetation is the amount of water that can be detained by vegetation canopy. This parameter is known as canopy storage capacity (Smax). During the quantification of interception loss, the canopy structure should be taken into account because it affects the water storage capacity of the canopy(Chen & Li, 2016). The storage capacity depends on the type of vegetation. Also, different landcover classes have different canopy structures and different morphology of leaves.

Furthermore, how much water can be stored, also depends on the shape of leaves and density of leaf area index(LAI), for instance, there is the difference in storage capacities between deciduous and conifers trees (Rutter, Morton, & Robins, 1975). The LAI is an important biophysical parameter that predicts the behavior of storage capacity of vegetation, especially for broad-leaved forests. Leaf Area Index as a parameter to account for the vegetation dynamics and it has been proven, to have a strong influence on canopy interception (van Dijk & Bruijnzeel, 2001). Also, based on an earlier study by De Jong & Jetten (2007) on the relation between LAI and Smax pointed out that each vegetation type has a unique relation.

Interception process in forested areas is an important linkage between the vegetation and hydrological cycle. Hence, the interception losses can have a significant impact on the water balance.
This study is aimed at quantification of rainfall interception loss of different land cover classes in the Veluwe area, the Netherlands using Sentinel-2 time series and remote sensing Gash (1979) model. Particularly, It will focus on monthly interception loss per land cover class and will also involve the analysis and temporal-spatial variation of leaf area index and fractional vegetation cover across the different land cover of the study area.

1.2. Research problem

The rainfall interception estimates using existing satellites is still insufficiently accurate. The rainfall intercepted by the canopy and its evaporation plays a crucial role in forest water balance. Remote sensing has been chosen as an alternative method for measuring the rainfall interception by forest (Cui et al., 2017).

However, because variation of interception, caused by different vegetation land cover types, estimating rainfall interception using remote sensing data from existing satellites of coarse resolution, still providing unreliable estimates. For example Miralles, Gash, Holmes, De Jeu, & Dolman (2010) estimated forest rainfall interception from multi-satellite, Vegas Galdos, Álvarez, García, & Revilla (2012) used Moderate Resolution Imaging Spectroradiometer (MODIS) to assess distribution of rainfall interception and Cui & Jia (2014) also used MODIS products to quantify rainfall interception loss of forest at regional scale.

Furthermore, some remote sensing (RS) parameters such as fractional vegetation cover (FVC) and Leaf area index (LAI) in many models are not frequently considered during interception modeling (Muzylo et al., 2009). Also, during rainfall interception modeling some models also do not consider the water evaporation during the rainfall (Mo, Liu, Lin, & Zhao, 2004), which leads to an underestimated value of rainfall interception loss.

Therefore, based on previous studies remote sensing method have not yet been used to estimate rainfall interception loss at this study area, particularly using observation products from Sentinel-2 as a new satellite with high resolution. This RS method will help us to estimate the interception loss of different land cover classes on a large area, and the accuracy will be tested by comparing estimates with field measurements. This present study, it will provide the reference for future research in the Veluwe area.

1.3. Main Objective

The main research objective is to quantify rainfall interception loss of different land cover classes on a large area using Sentinel-2 time series in the Veluwe area.

1.3.1. Specific Objectives

- To assess the temporal and spatial variation of LAI across different landcover at the Veluwe area.
- To assess the temporal and spatial variation of Fractional vegetation cover across different landcover at the Veluwe area.
- To estimate rainfall interception loss of different land cover classes at the Veluwe area using Sentinel-2 time series combined with RS-Gash model.
- To quantify the relationship between the leaf area index and Interception loss at the Veluwe area.

1.4. Research questions

- What is the temporal and spatial variation of LAI across landcover types in the Veluwe area?
- What is the temporal and spatial variation of Fractional vegetation cover across different landcover in the Veluwe area?
- How can the observations from Sentinel-2 be used to estimate monthly rainfall interception loss of different types?
- What is the relationship between the leaf area index and Interception loss?

1.5. Thesis outline

Section 1 is the introduction including the background, research problem, main objectives, specific objectives, and research questions. Section 2 reviews related works conducted to have more insights on the methodologies so that can be applied in this research. Section3 describes the study area about location, size, and land use. Section 4 describes data sources, data types and other data used in this research.

Section 5 presents the flow chart of different methods and data pre-processing approaches to obtain different data used. Section 6 presents the results from data pre-processing and their analysis. Section 7 discusses the obtained results, their relevance to the study area and conclusions. The section gives some recommendations to the future study.

2. LITERATURE REVIEW

2.1. Rainfall Interception

Precipitation can be considered as the major parameter that controls the hydrological cycle of the region (De Jong & Jetten, 2007). In hydrology, precipitation is always considered as the start of the hydrological cycle. However, in the forest, during the rainfall process, some rainwater directly falls on the ground through the space between trees or temporally being retained by the leaves and then drip off, which is called throughfall. Other rainwater either reaches the ground along the stem of the tree which is represented as stemflow and eventually evaporates back to the atmosphere. The portion of rainfall being captured is the one called rainfall interception (Crockford & Richardson, 2000) while the part that is stored in the canopy is called interception storage capacity and the other stored in the stems is called trunk storage capacity.
Interception loss can be expressed as the volume of rainwater evaporated from the wetted canopy cover during a specified duration (Bakar, Bin Baki, Bt Hamzah, Bin Yusop, & Bin Khalil, 2012).

The total amount of rainfall intercepted, stored and eventually lost through evaporation is considered to be a canopy interception loss. The intercepted water always recharges the storage of forest canopy and discharged by evaporation and drip (Massman, 1983). Therefore interception loss affects the forest water balance where intercepted rainwater evaporates back to the atmosphere without replenishment of soil moisture and groundwater recharge. It is crucial to know the interception loss because, it improves the modeling of regional, global water balances and understanding the terrestrial water cycle processes (Cui & Jia, 2014). In hydrological models, the interception by vegetation is an essential factor where it accounts for 10 to 20% of total precipitation (Oerlemans & Vink, 2010). Therefore for reliable results in the quantification of forest water balance, interception models are essential to understanding interception processes (Muzylo et al., 2009).

The first attempt to estimate rainfall interception loss using the conceptual model was made by Horton, (1919). By 1970s interception loss had been estimated empirically by the difference between gross rainfall and net rainfall (Muzylo et al., 2009). After Horton's work, the first conceptual model describing interception as a process driven by evaporation was followed by Rutter, Kershaw, Robins, & Morton (1971). In the same century next model was Rutter et al. (1975), almost ten years after original Rutter model, Gash (1979) developed the first analytical interception model to estimate rainfall interception by forests, this Gash model provided a simplified solution to the Rutter model (Muzylo et al., 2009).

According to the review of rainfall interception models done by Muzylo et al. (2009), Gash Analytical interception model was among the first approved models with outstanding performance. However, Gash (1979) model calculates rainfall interception loss of trunk and canopy separately, which requires more parameters such as mean evaporation rate from the canopy (E_C), mean rainfall rate ($\bar{R}$), canopy cover (C), Unit canopy capacity (S_C), trunk storage capacity (S_t) and stemflow (Pt) coefficient. In addition, some parameters such as trunk storage capacity and the amount of rainfall falls along the tree stem are difficult to estimate at the regional scale (Cui & Jia, 2014). In this study, the remote sensing (RS) Gash model was suggested to simplify the Gash (1995) model.

2.2. Sentinel-2 Optical Satellite images

Sentinel-2 is a multiple spectral sensor launched in June 2015 through Global Monitoring for Environment and Security (GMES) in partnership with ESA. This Satellite comprises of two satellites; Sentinel-2A launched 23rd June 2015 and Sentinel-2B launched 7th March 2017. The images have spatial resolution 10m, 20m, and 60m with a swath width of 290 kilometers. The images can be acquired and accessed online through the European space agency (ESA) scientific hub website. Sentinel-2 images can be used in different applications for monitoring of spatial planning, water, and forest monitoring (Baillarin , Meygret , Petrucci , Lacherade , Tremas , Isola , Martimort, 2012, ESA, 2015).

Furthermore, Sentinel-2 is very powerful due to its high spatial resolution and multi-spectral information, with 13 spectral bands (Table 2-1) and a ten day revisit time for one sensor (Baillarin , Meygret , Petrucci , Lacherade , Tremas , Isola , Martimort, 2012). The visible and near-infrared bands have 10m spatial resolution for land application , 4 vegetation red edge bands has 20m spatial resolution and 2 SWIR bands which have 20m spatial resolution for snow, ice , and cloud detection (Figure 2-1), 3 bands of 60m spatial resolution for atmospheric correction and cirrus detection (Baillarin , Meygret , Petrucci , Lacherade , Tremas , Isola , Martimort, 2012) Also, Sentinel-2 has a high temporal resolution of 5 days with two satellites, and it captures the information covers all coastal and land areas between 84°N and 56°S crossing the equator at 10:30 a.m the local time (Mandanici & Bitelli, 2016, ESA, 2015).

Table 2-1: Sentinel-2 spectral bands with its Resolution

Sentinel-2 Bands	Central wavelength (μm)	Resolution (m)
Band 1-Coastal aerosol	0.443	60
Band 2- Blue	0.490	10
Band 3- Green	0.560	10
Band 4- Red	0.665	10
Band 5- Vegetation Red-edge	0.705	20
Band 6- Vegetation Red -edge	0.740	20
Band 7 -Vegetation Red -edge	0.783	20
Band 8- NIR	0.842	10
Band 9 -Water vapour	0.945	60
Band 10 -SWIR-Cirrus	1.375	60
Band 11 -SWIR	1.610	20
Band 12- SWIR	2.190	20

Source: (ESA, 2015)

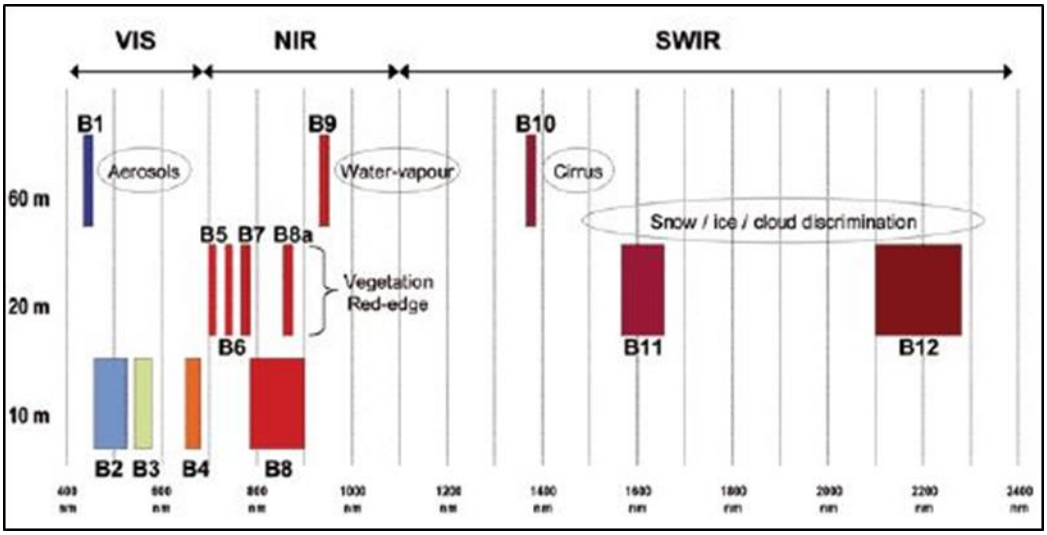

Figure 2-1: Sentinel-2 bands arrangement and their use Source:(ESA, 2012)

2.3. Corine Landcover (CLC)

Corine Landcover (CLC) was created by many countries in Europe using visual interpretation method of high satellite images through identifying and assessing objects recorded in aerial or satellite images. The CLC was specified in the 1980s to standardize data collection on land in Europe and to provide information on the biophysical characteristics of the earth surface (Barbara Kosztra, György Büttner, Gerard Hazeu and Stephan Arnold, 2017). It was invented in 1985, and current updates were produced in 2000, 2006, and 2018. It consists of 44 classes of invented land cover. The current version CLC 2012 covers 39 European Environmental Agency(EEA)countries. CLC normally uses the minimum mapping unit(MMU) of 25ha (500 * 500 m) for real phenomena and a minimum width of 100m for linear phenomena. The 2012 version of CLC is considered as the first one fixing the CLC time series in Copernicus programme; hence it ensures the sustainability for future use. The CLC products are available in both raster and vector format (100 and 250-meter spatial resolution).

3. DESCRIPTION OF THE STUDY AREA

The Veluwe is a forest-rich ridge of hills in the central part of the Netherlands, and it is in the western part of Gelderland province. The Veluwe forest is one of the largest protected areas in the country covering 55 00 ha of forest and heather, the most notable feature of this area is the existence of hilly ranges. It comprises approximately 613 ha of deciduous forest, 2282 ha of coniferous forest and drift sand which is one of the largest reserved nature in the Netherlands (Hein, 2011). The large part of Veluwe is assigned as a National Nature Reserve. Furthermore, the Veluwe area is populated with cities such as Apeldoom, Arnhem, Amersfoort, Deventer, Zwolle, Harderwijk and Zutphen. In this study, the shapefile of different land cover classes of the study area (Figure 3-1) was downloaded from the Corine Land Cover website of the European Environment Agency (2012).

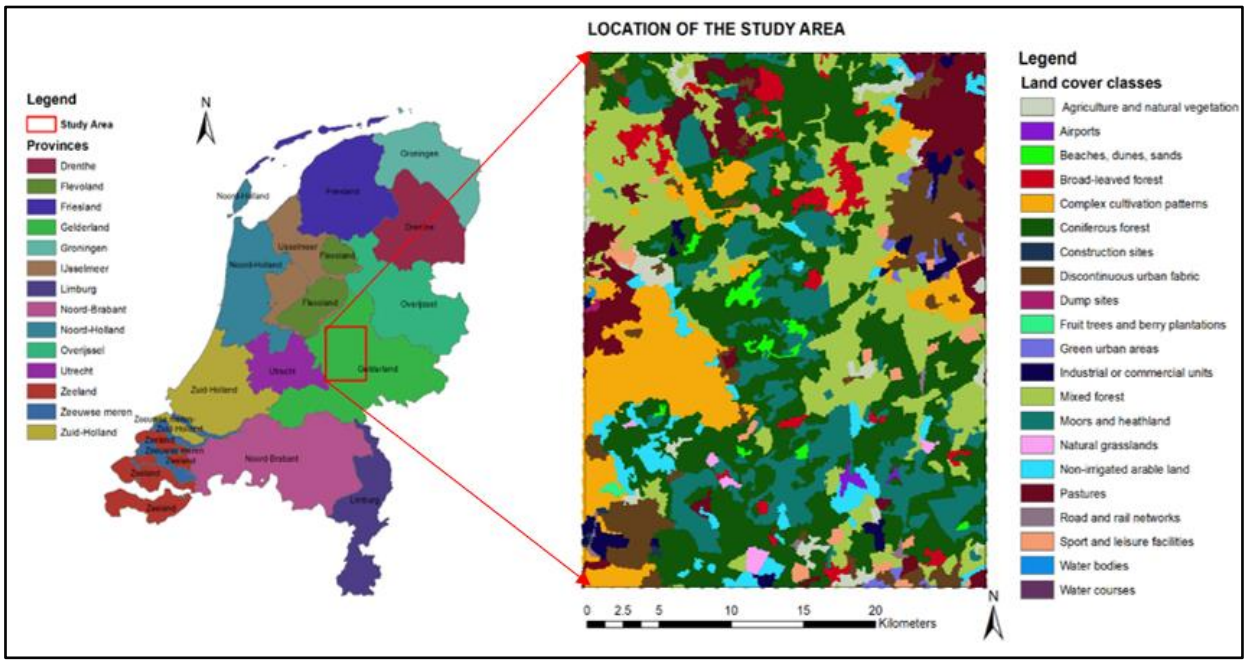

Figure 3-1: Location of study area

3.1. Land use and vegetation

In the past, the pastures were concentrated in the lowlands around the Veluwe area. By the Mid-eighteenth centuries, the Hoge Veluwe comprised the entire part of drifting sand, and heathlands were only ten percent consists of forest and agriculture area. However, due to the intensive use of the heathlands for tending sheep and cutting of heathsods leads to the renewal of sand drift hence the disappearing of local vegetation and former Pleistocene covering the sand were eroded by the wind (Dijkshoorn, 2017). Since the end of the 19th century, heathlands were no longer used for the tending of sheep, and there was no more cutting of heath sods. Therefore, the large areas of wind-blown sands are now forested where most of the central Veluwe is covered with forest with a relatively small area of heath and grasslands (Hein, 2011).

4. DESCRIPTION OF THE DATA SOURCES

4.1. Meteorological data

Hourly climatic data include rainfall, global radiation, average air temperature were accessed from the archive of Royal Netherlands Meteorological Institute (KNMI). Hourly rainfall data, global radiation and temperature from January 01st to December 31st from stations of De Bilt, Lelystad, Deelen and Heino were acquired from the KNMI: https://www.knmi.nl/nederland-nu/klimatologie/uurgegevens

Table 4-1: Location of rainfall stations

Station names	Station number	Coordinates		Elevation above NAP (m)
		Longitude	Latitude	
De Bilt	260	5.180	52.100	1.90
Lelystad	269	5.520	52.458	-3.70
Deelen	275	5.873	52.056	48.20
Heino	278	6.259	52.435	3.60

4.2. Remote sensing data

Sentinel-2 time series images at a 20m spatial resolution in the SAFE format were acquired from June to December (excluding the month of November, because the whole image of this month was completely affected by clouds) from the following web site: https://scihub.copernicus.eu/. Leaf area index (LAI) and Fractional Vegetation cover (FVC) were processed from time series of six images only which were more or less cloud free. The study area was the subset from the main image of the Sentinel-2.

Table 4-2: Downloaded time series images

Number	Identification	Dates
1	MSIL1C_UFT_20160607T104026	07/06/2016
2	MSIL1C_UFT_20160720T105547	20/07/2016
3	MSIL1C_UFT_20160826T104023	26/08/2016
4	MSIL1C_UFT_20160925T104115	25/09/2016
5	MSIL1C_UFT_20161005T104018	05/10/2016
6	MSIL1C_UFT_20161227T105527	27/12/2016

4.3. Corine Land cover

A map of the selected land cover classes was prepared using Corine land cover (CLC). CLC raster shapefile of 100m spatial resolution was downloaded from the Corine Land Cover website of European Environment Agency (2012). The current version of CLC 2012 covers 39 European Environmental Agency (EEA) countries was used in this study. The analysis of CLC 2012 over 100% coverage for each country of the EEA39 was performed, and the overall accuracy in the Netherlands was 89.20% (Jaffrain, 2017).

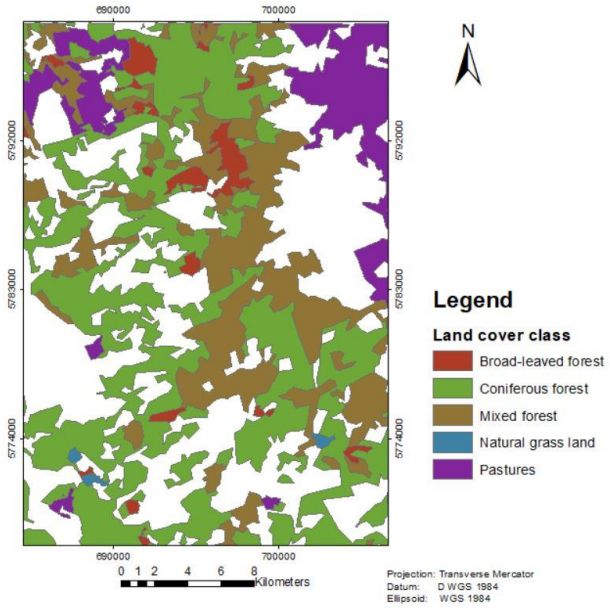

Figure 4-1: Five selected land cover classes with their suface areas

Therefore the raster shapefile of different land cover classes of the study area was extracted, and five land cover classes were selected for this present study.

Table 4-3: Selected land cover class with their classification codes

CLC Code	Land cover classes	Area(ha)
311	Broad-leaved forest	2765
312	Coniferous forest	28225
313	Mixed forest	17153
321	Natural grassland	422
231	Pastures	8004

4.4. Other data used

The field data (June to October 2016) of rainfall interception loss at Speulderbos site from the previous study by Cisneros et al. (2018) graduated PhD student in Department of Water Resources, ITC was used to compare estimated interception loss of the present study for the case of the coniferous plot. The Speulderbos site is part of Veluwe area with coniferous-fir of 2.5 ha tree density where Flux tower of 47.4m height is installed. The comparison between the estimated and measured interception was only on the plot of coniferous forest, and the key parameters considered include Leaf area index, canopy storage capacity, mean rainfall rate, mean evaporation rate, and fractional vegetation cover.

5. RESEARCH METHODOLOGY

5.1. Methodology Flowchart

Figure 5-1 shows the overall methodology flow chart. The mean precipitation data, mean evaporation, vegetation storage and fractional vegetation cover (FVC) are input parameters to the model. First, the raw data Sentinel-2 images and Meteorological data were pre-processed. Sentinel-2 Level-1C were downloaded from Copernicus scientific hub. Thus, Level-1C images were converted (atmospheric correction) using Sen2cor plugin in SNAP 6.0 version (Sentinel application platform) to Level-2A (bottom of the atmosphere). Thus, further data pre-processing procedures (Figure 5-2) was followed.

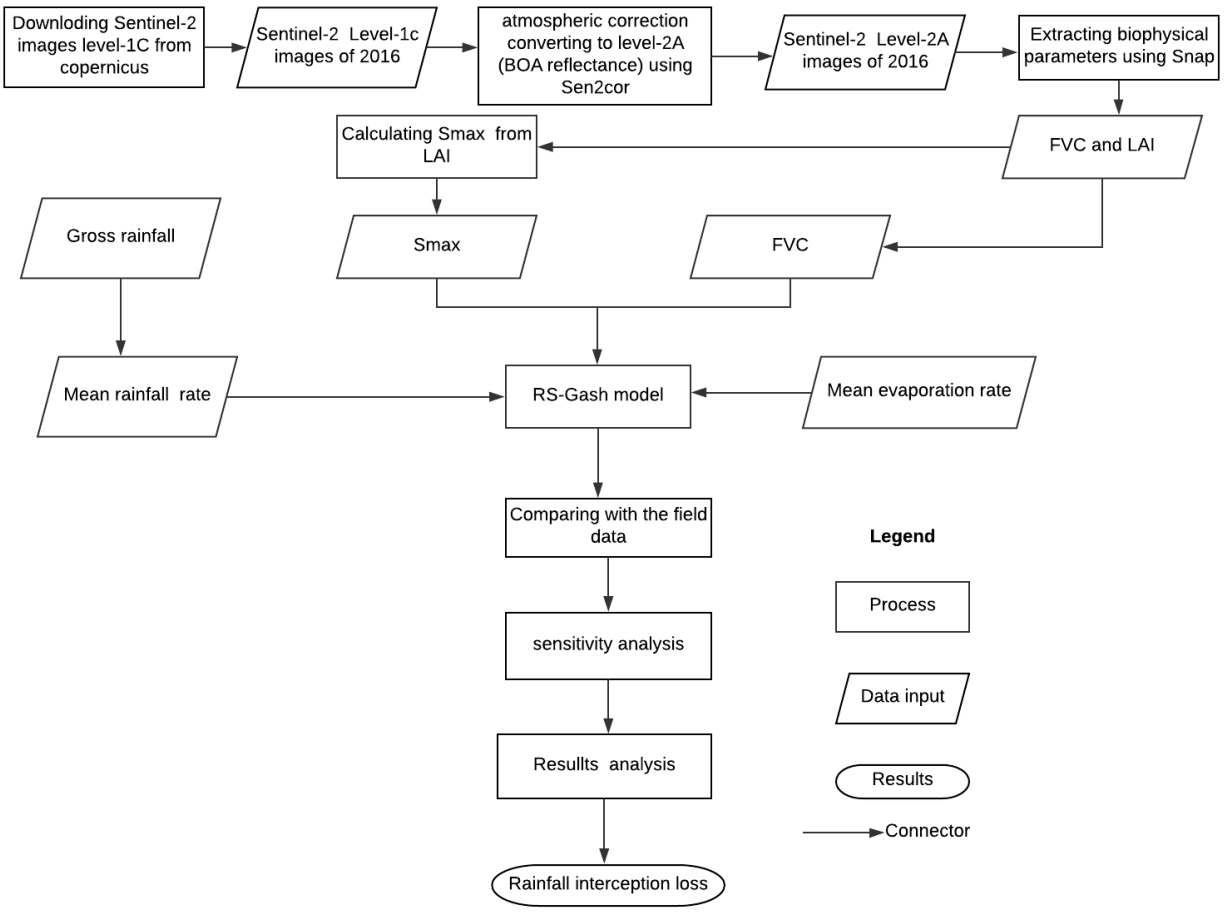

Figure 5-1: Methodology flowchart

5.2. Remote sensing Gash model

The Remote sensing (RS)-Gash model by Cui & Jia, (2014) was used to estimate rainfall interception (I, mm). RS-Gash model was suggested to simplify the Gash (1995) model in order to estimate the interception loss of different landcover classes using remote sensing method on large scale.

Table 5-1: Terminology used in RS-Gash model

Names	Definition	Symbol used	Unit
Gross rainfall	Rainfall measured in the open area closer to the study area or above the forest canopy	Pg	mm
Threshold rainfall	The amount of rainfall responsible to saturate the vegetation canopy	Pg'	mm
Mean rainfall rate	Mean rainfall rate from the saturated canopy	$\bar{R}$	mm/hr
Mean evaporation rate	Mean evaporation per unit ground area	$\overline{EV}$	mm/hr
Fractional vegetation cover	The ratio of the vegetation occupying a unit area	FVC	%
Vegetation storage	Vegetation storage capacity per unit area of ground	$Sveg$	mm
Canopy storage capacity	Amount of rainwater can be detained by vegetation	$Smax$	mm
Leaf area index	The ratio of total upper leaf surface of vegetation to the surface area of the land on which vegetation grows.	LAI	m^2/m^2

5.3. Data pre-processing

Figure 5-2 shows the whole procedure for pre-processing of downloaded sentinel-2 multi-spectral imagery(MSI) products and extraction of LAI and FVC. The Sen2cor plugin in SNAP (Sentinel application platform) was used to correct images (atmospheric correction) where level-1C images were converted into Level-2A bottom of atmosphere reflectance. Also, the images were cut to the extent of the study area using a subset function in SNAP (http://step.esa.int/main/toolboxes/snap/). After that, ArcGIS was used for images projection, preparation, and calculating LAI and FVC values of different land cover using zonal statistics tool. The acquisition date of images was supposed to be between January and December 2016, but because of many images were much affected by clouds, only six images from June to December 2016 were obtained with discontinuity of November, due to the problem of clouds.

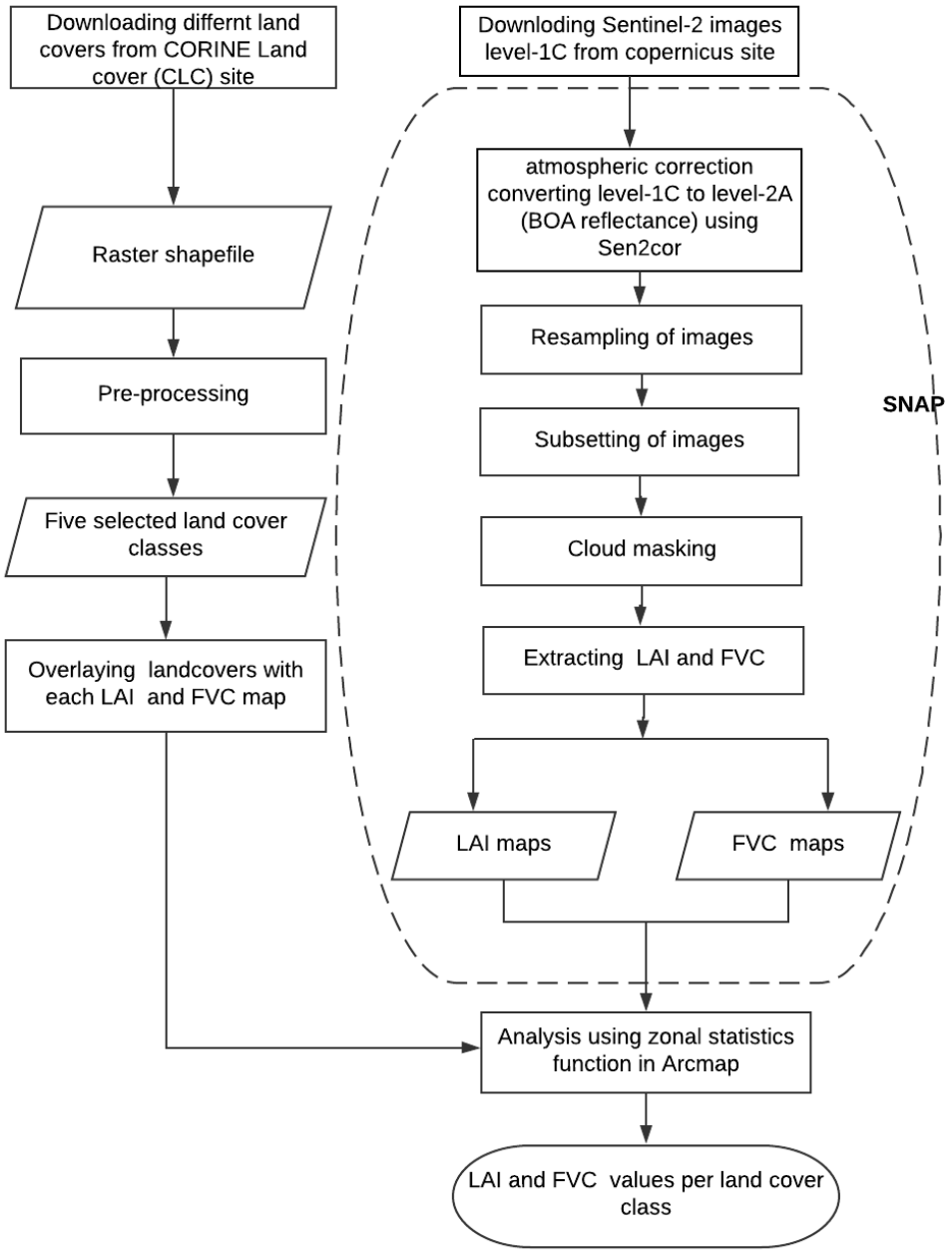

Figure 5-2: Data pre-processing flow chart

5.3.1. Subsetting of Sentinel-2 imagery

Before subsetting, resampling operation was done to all the images, so that all the bands have the same size. Then Sentinel-2 images of Level-2A were subsetted according to the extent of study area boundary.

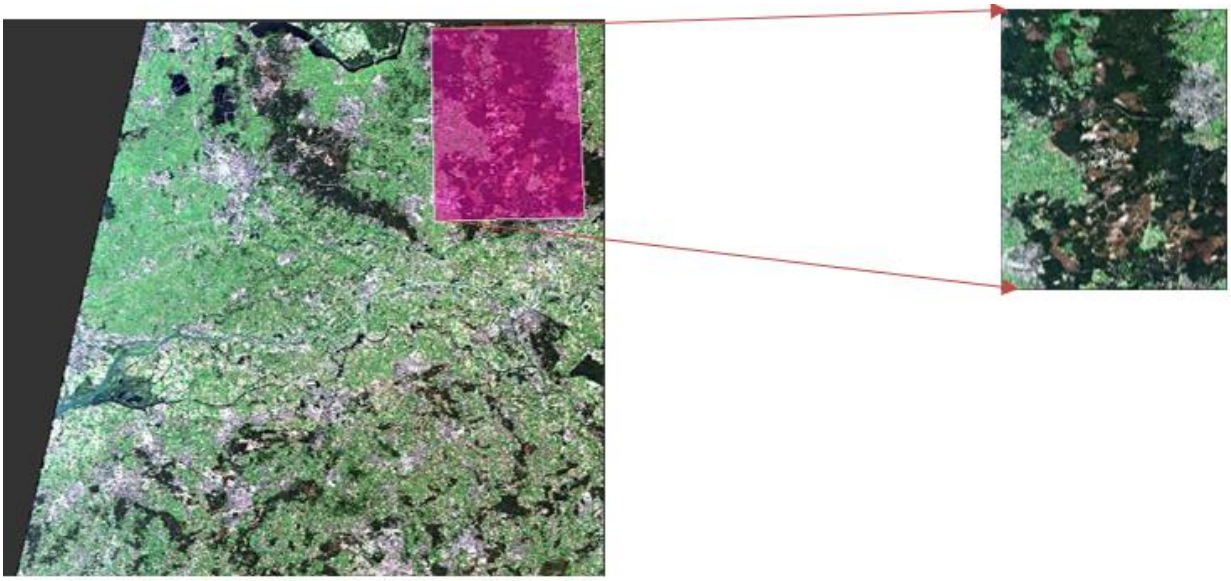

Figure 5-3: Granule subset of study area from Sentinel-2 image using subset function in SNAP

5.3.2. Leaf Area Index (LAI)

Rainfall interception can be estimated using remote sensing based on vegetation indices such as Fractional vegetation cover, Normalized difference vegetation index and Leaf area index as a biophysical parameter (Vegas Galdos et al., 2012).
LAI is one of the most common parameters used for vegetation change and based on previous literature; LAI is a biophysical parameter which was proven to have a strong correlation with canopy interception (van Dijk & Bruijnzeel, 2001). LAI can be defined as the ratio of total upper leaf surface of vegetation to the surface area of the land on which vegetation grows.

It is an important surface biophysical parameter as a measure of vegetation cover and vegetation production in general. In the present study, LAI was extracted from Sentinel-2 images of the study area where the image of each month (June to December 2016) was processed using the biophysical processor of SNAP. The series of images had the discontinuity in November because the November image was seriously affected by clouds. Also, the scale of 0 to 8 maximum LAI value was fixed in SNAP for quality checking of temporal variation of LAI and to remove pixels with negative numbers and erroneous values due to clouds that causing the spikes as shown in the histogram (Figure 5-4).

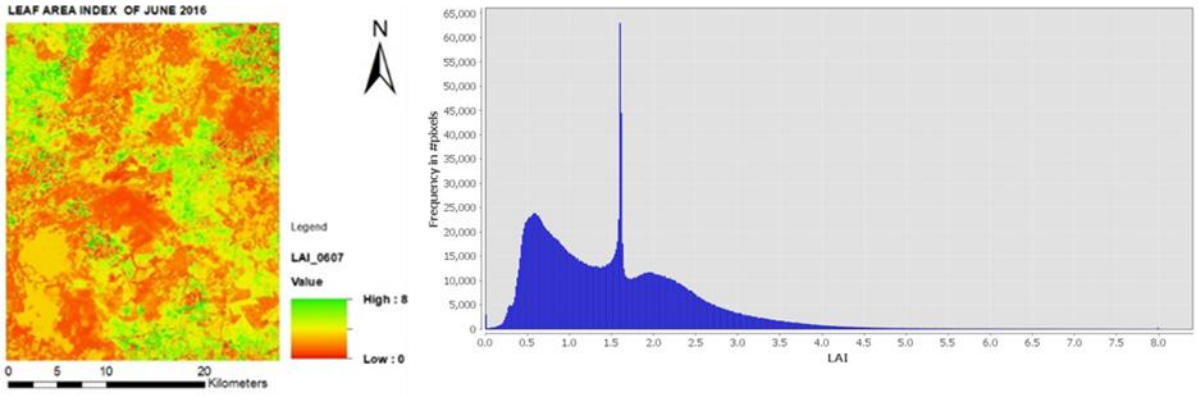

Figure 5-4: sample of images with histogram showing spikes

The LAI of each month was obtained (Figure 6-1). Image masking was done based on logical band maths expression algorithm identifying pixel by pixel in mask manager of SNAP software. The pixels affected by clouds, dark shadows, thin cirrus and dark features (Figure 5-5) were masked out and became no data (Figure 5-6). "Cloud masks identify cloudy pixels and separate them from those that are cloud-free"(Coluzzi, Imbrenda, Lanfredi, & Simoniello, 2018).

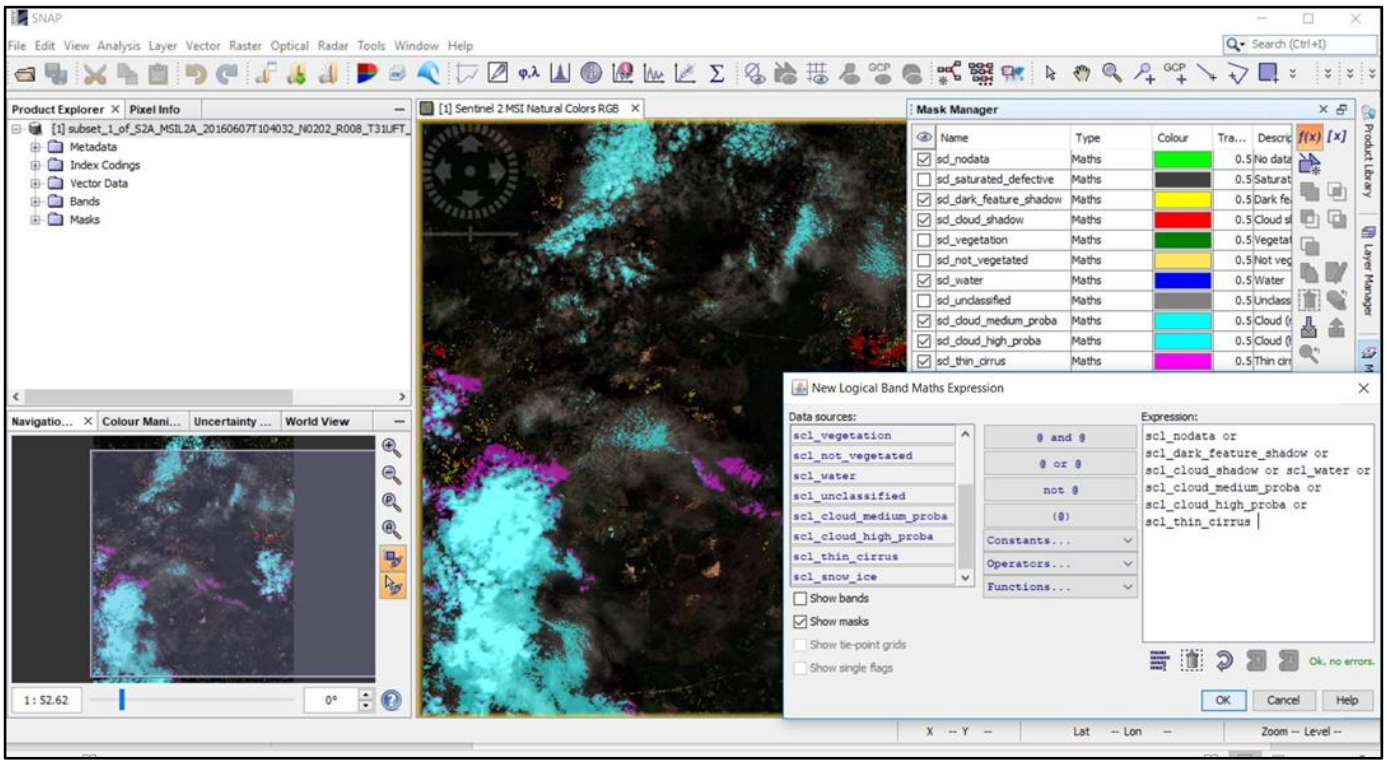

Figure 5-5: Cloud masking process

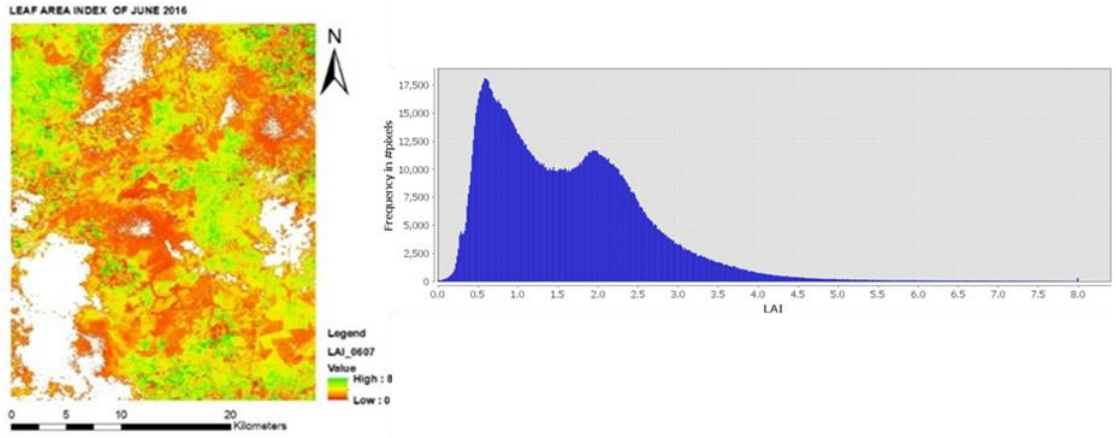

Figure 5-6: Sample of images showing areas with no data pixels after cloud removal

After cloud free, LAI map of each month was crossed with land cover shapefile of the study area, and LAI value per each land cover was obtained.

5.3.3. Fractional Vegetation cover (FVC)

Fractional Vegetation cover is the ratio of vegetation occupying a certain unit area. It is a crucial parameter that indicates the nature of land by separating non-vegetated, partially vegetated and densely vegetated land surfaces (Song et al., 2017). In this study, FVC was processed from sentinel-2 images using the biophysical processor of SNAP software after cloud masking where clouds, dark shadows, thin cirrus, and dark features were removed from each image using logical band maths expression algorithm in mask manager of SNAP software. After the cloud-free FVC map of each month was crossed with land cover shapefile then the FVC value of each land cover was obtained.

5.3.4. Canopy storage capacity

Canopy storage capacity is the key parameter in interception models and is defined as the amount of rainwater can be detained by vegetation. It is an essential parameter because different vegetation types have different canopy structures and different morphology of the leaves (De Jong & Jetten, 2007). Rainfall interception loss can be divided into two parts: interception loss by canopy and tree trunk (Calder, 1998). Vegetation storage capacity includes canopy storage capacity and trunk storage capacity. Therefore, Canopy storage capacity is crucial because sometimes the trunk is very small and the rain can only reach the trunk when the rainfall is too much (Gash, Lloyd, 1995).

However, in this study, the canopy storage capacity of each land cover class was calculated from LAI based on Vegas Galdos et al. (2012) equation below .

$$S_{max} = f * ln(1 + LAI) \quad (1)$$

Where f is the specific factor depending on the vegetation type , $Smax$ (mm) is the canopy storage capacity and LAI is the leaf area index in ($m^2.m^{-2}$). According to the study by Vegas Galdos et al. (2012) f values in the table were optimized for each land cover class.

Table 5-2: Factor f value per land cover class adopted from Vegas Galdos et al. (2012)

Land cover class	f values
Broad-leaved forest	1.6
Coniferous forest	2
Mixed forest	1.6
Natural grassland	1
Pastures	1

Table 5-3: Monthly canopy storage capacity per land cover class calculated from mean LAI

Period	Land cover classes				
	Broad-leaved forest	Coniferous forest	Mixed forest	Natural grassland	Pastures
JUN	1.90	1.94	1.82	1.03	1.07
JUL	2.12	2.33	2.01	1.16	1.08
AUG	1.98	2.19	1.89	1.09	0.92
SEP	1.86	2.02	1.76	0.97	0.71
OCT	1.75	1.93	1.69	0.90	0.64
DEC	0.60	1.21	0.90	0.65	0.29

5.3.5. Rainfall and Mean rainfall rate

First, the interpolated hourly gross rainfall data (01st January to 31st December 2016) from four automated KNMI stations closest to the study area were acquired from the Department of Water Resources, ITC. The only gross rainfall of six months (June, July, August, September, October and December) were selected in order to match with time series of other data.

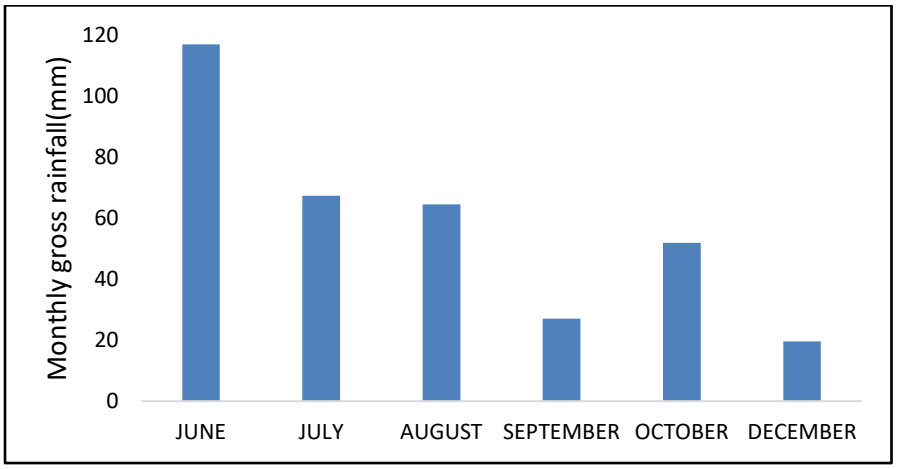

Figure 5-7: Monthly gross rainfall from June to December 2016

Mean rainfall rate ($\bar{R}$) was obtained by calculating average rainfall (considering only hourly rainfall rate greater than 0.5 mm/hr) in each month per station (Table 5-4). After, only six months(June, July, August, September, October and December) were selected excluding the month of November regarding to the time series of other model in puts . Therefore, Inverse distance Weighting (IDW) interpolation method was used to interpolate mean rainfall from four stations. After, Interpolated map of rainfall intensities of each month (June to December 2016) was overlaid with the shapefile of different land cover classes and monthly rainfall rate (mm/hr) per land cover class was obtained.

Table 5-4: Mean hourly rainfall rate per month from June to December 2016

Station No	Station name	June	July	August	September	October	December
260	De Bilt	3.04	1.88	1.58	1.28	1.34	0.85
269	Lelystad	2.08	2.50	1.91	2.37	2.21	1.09
275	Deelen	2.62	2.90	1.58	3.80	2.85	0.98
278	Heino	1.94	1.54	1.74	1.52	2.88	1.15

5.3.6. Mean evaporation rate

Evaporation of the present study was calculated using Makkink reference evaporation (Hiemstra & Sluiter, 2011). Makkink's method requires average air temperature and incoming shortwave radiation.

It is mostly used in the Netherlands. The climatic data were obtained from four automated KNMI stations closest to the study area. The evaporation is calculated using the Makkink reference evaporation method as follows:

$$ET_{ref} = C.\frac{s}{s+\gamma}.\frac{S^{\downarrow}\text{day}}{\lambda*\rho} \quad (2)$$

where ET_{ref} (m/day), is the Makkink reference evaporation, C is a constant equal to 0.65 , s (kPa/°C) is the slope of the saturation curve of water vapor pressure, γ (kPa/°C) is the psychometric constant, $S^{\downarrow}_{day}$ (J/m^2/day) is the daily incoming radiation, and ρ is the bulk density of water equal to 1000kg/m^3.

$$s = \frac{7.5*237.3}{(237.3+T_{day})^2} * ln10 * e_s \quad (3)$$

$$e_s = 0.6107 * 10^{\frac{7.5\,T_{day}}{237.3+T_{day}}} \quad (4)$$

$$\gamma = 0.0646 + 0.00006 * T_{day} \quad (5)$$

$$\lambda = (2501 - 2.375 * T_{day}) * 1000 \quad (6)$$

where e_s (hpa) is the saturation vapour pressure, γ (hpa) is psychrometric constant and λ is the heat of the vaporization.

According to the present study, the hourly incoming radiation ($S^{\downarrow}_{hour}$) and temperature(T_{hour}) were obtained from four KNMI meteorological stations. To calculate the mean evaporation rate in each month was obtained from each of four stations.

Table 5-5: Monthly mean evaporation rate ($\overline{EV}$) from June to December 2016

Station No	Station name	June	July	August	September	October	December
260	De Bilt	0.109	0.086	0.095	0.041	0.034	0.000
269	Lelystad	0.066	0.107	0.089	0.059	0.025	0.000
275	Deelen	0.057	0.129	0.089	0.046	0.029	0.000
278	Heino	0.610	0.963	0.645	0.553	0.293	0.002

Interpolation of the mean evaporation rate from four stations was performed, and interpolated mean evaporation rate map of the study area was obtained. After each monthly mean evaporation rate map was overlaid with the shapefile of different land cover classes and mean evaporation rate per land cover class was obtained.

5.4. Modelling rainfall interception

The practical application of RS-Gash model requires the definition of each state variable shown in

Table 5-1. The parameters such as LAI and FVC were obtained by remote sensing technique while other parameters were derived using other methods as explained before. RS-Gash model is based on rainfall events as in original analytical Gash, (1979) model. It is very important to carry out the event based analysis because the way used to separate events might have a major impact on the modelling of rainfall interception Cisneros, Tol, & Ghimire, (2018).

First, the rainfall was separated into a series of events for each month. After, the event with at least 0.5mm of rainfall was defined. Also, the events were separated whereby at least three hours after the rainfall terminated were considered as the complete drying up of the canopy (Klaasen, Bosveld, & de Water, 1995). Saturated events were defined only for the events with the Pg>0.5mm/hr preceded by at least 3 hours of dryness (Klaassen, Bosveld, & de Water, 1998) .

The rainfall necessary to saturate the vegetation (Pg') was estimated according to Cui & Jia (2014)

$$Pg' = -\frac{\bar{R}}{\overline{E_V}} * \frac{S_{veg}}{FVC} * \ln\left(1 - \frac{\overline{E_V}}{\bar{R}}\right) \quad (7)$$

s_{veg} is the vegetation storage capacity in (mm) that includes both canopy and trunk storage capacity and it is assumed to be linearly related with vegetation area. However, in the present study $Smax$ (canopy storage capacity) in (mm) defined as the amount of rainwater that can be retained by vegetation was adopted to replace s_{veg}. $Smax$ of each land cover type was calculated from leaf area index in (Eq.1) according to Vegas Galdos et al. (2012).

Based on the canopy saturation the rainfall interception loss per landcover was estimated using the following equations

For low rainfall that cannot saturate the canopy storage, where $Pg < Pg'$

$$I = FVC * Pg \quad (8)$$

For high rainfall that can saturate the canopy storage, where $Pg > Pg'$

$$I = FVC * Pg' + \left(FVC * \frac{\overline{E_V}}{\bar{R}}\right)(Pg - Pg') \quad (9)$$

Where I is interception loss in (mm), $\overline{EV}$ is the mean evaporation rate per unit vegetation coverage area in (mm/h) including evaporation rate from canopy and stem; $\bar{R}$ is the mean rainfall rate in (mm/h), Pg is the gross rainfall in (mm).

6. RESULTS

6.1. Spatial and temporal variation of Leaf area index across landcover types from June to December 2016

First, the monthly LAI maps from June to December 2016 with discontinuity of November at a spatial resolution of 20 m were derived for this study using Sentinel-2 images (Figure 6-1). The study area shows a high density of LAI in August and September and low density in December. There is the effect of clouds, for instance in June and October, these clouds had an impact on LAI values, during the cloud removal, affected pixels were removed and leave the holes with no data. For instance, LAI map of June clearly shows holes with no data value.

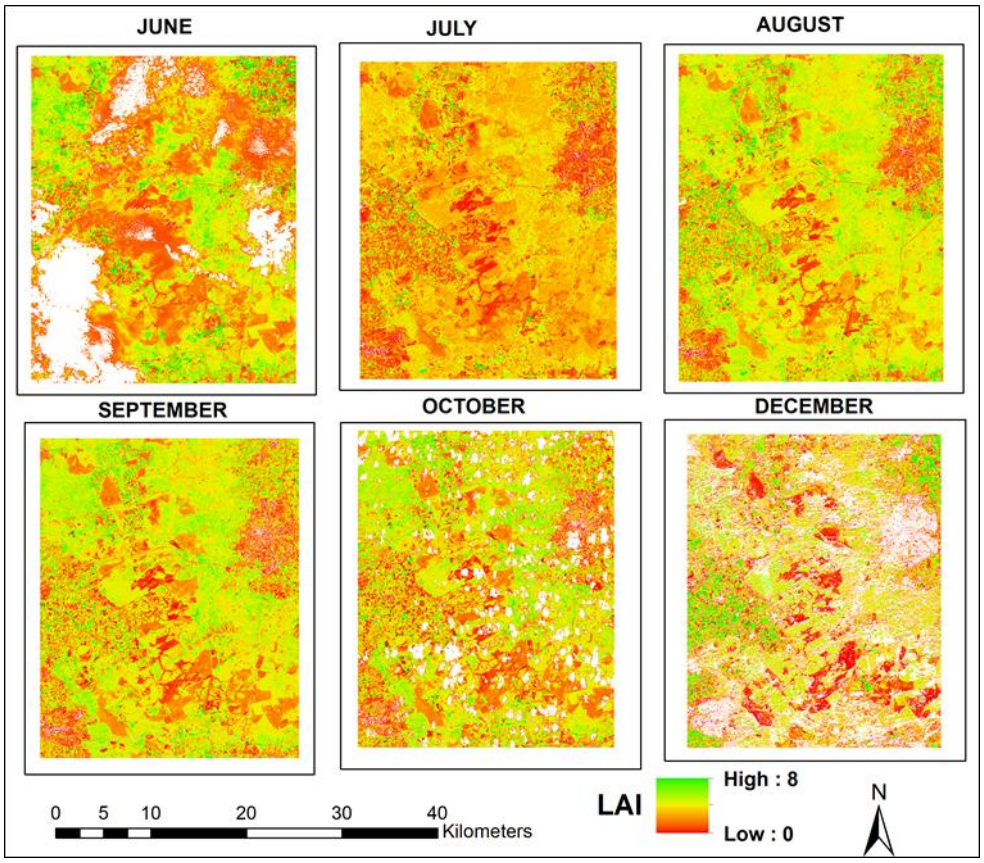

`

Figure 6-1: Spatial variability of LAI from June to December 2016

In this study, the mean LAI value in the whole season (from June to December 2016) range from 0.3 to 2.8 as presented in the box plot (Figure 6-2). The broadleaf forest has the highest mean LAI value while natural grassland has the lowest mean LAI.

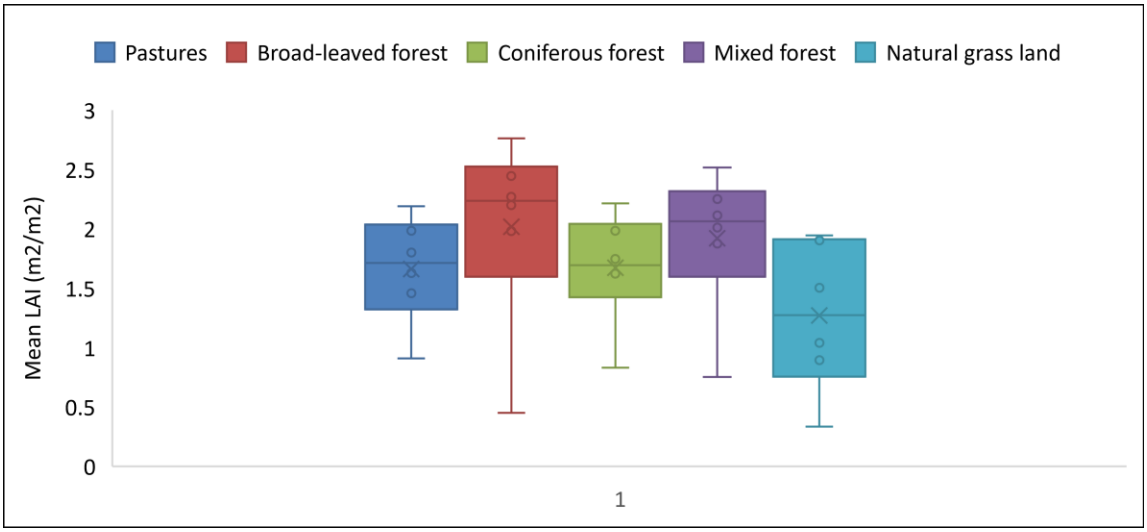

Figure 6-2: Mean LAI, median, first and third quartile, the minimum and maximum value (from June to December 2016) over the pixels of each land cover class.

From Figure 6-3 below shows the monthly maximum LAI values over the pixels of each land cover. The most landcover classes of pixels with maximum values are found in both June and July corresponding to pastures, broadleaf forest, coniferous forest, and mixed forest.
On the other hand, the lowest LAI values were found in December for some pixels of broadleaf forest and grassland according to the value range (from 0 to 8) used in this study.

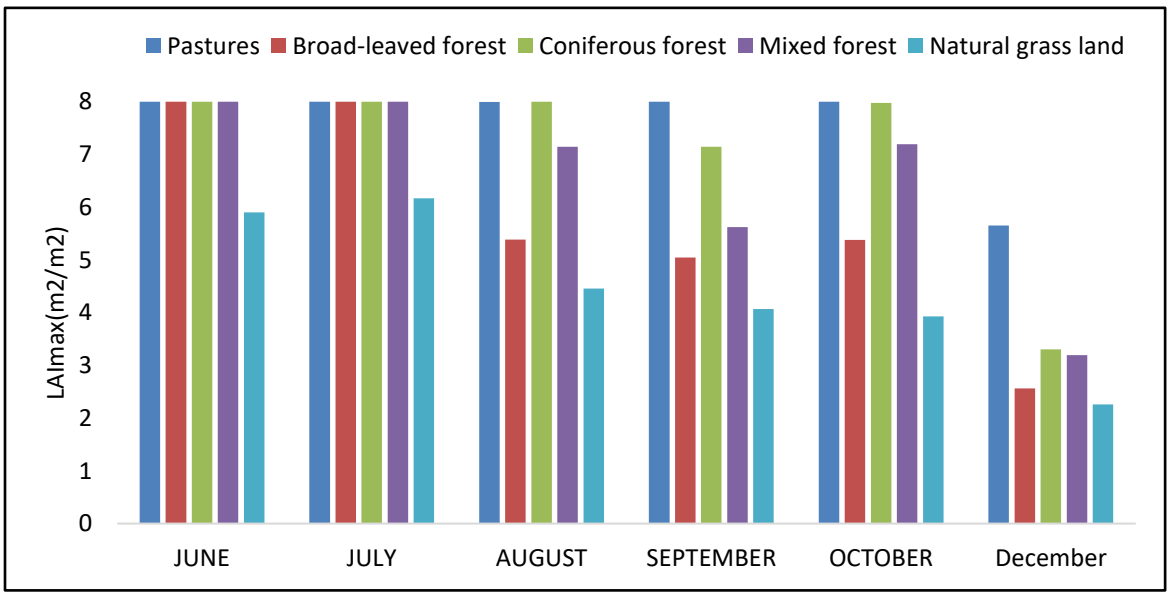

Figure 6-3 : Temporal pattern of maximum LAI value per land cover class from June to December 2016

6.2. Spatial and Temporal variation of Fractional Vegetation Cover (FVC)

The fractional vegetational cover (FVC) varies from 0 to 1 with the monthly mean value between 0.11 and 0.66 over the study area correspond to 11% and 67% respectively as presented in Figure 6-4. The most pixels with a high percent of fractional vegetation cover are found in July and August correspond to natural grassland, pastures, mixed forest, and broadleaf forest, i.e., Coniferous forest has the lowest FVC among the other land cover types in July and August.

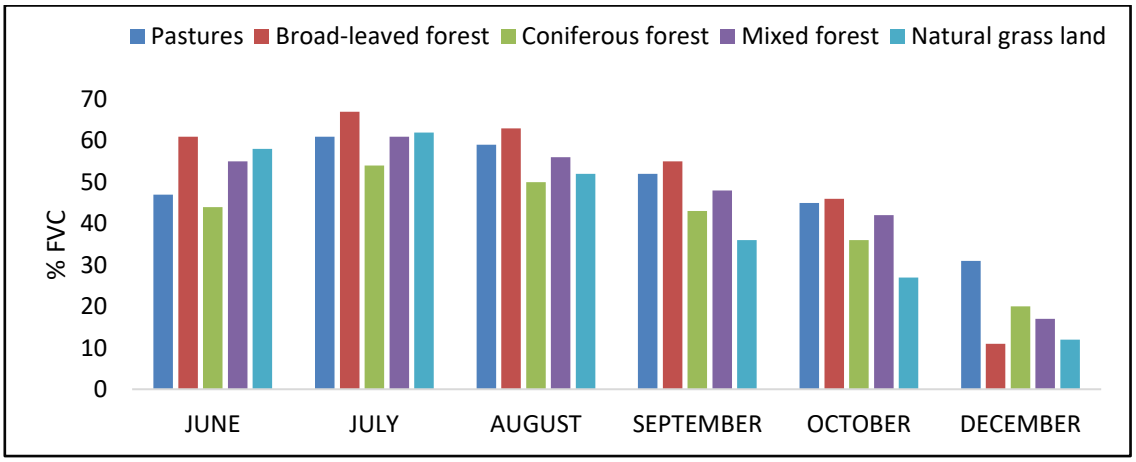

Figure 6-4: Temporal pattern of mean Fractional vegetation cover over the pixels per land cover class from June to December 2016

Based on Figure 6-5, there is a significant temporal variation of FVC over the study area. The most vegetated areas are found in July and August. Also, there is an influence of cloud removal to the gradual decrease of FVC. For instance, most low FVC values are found in October and December.

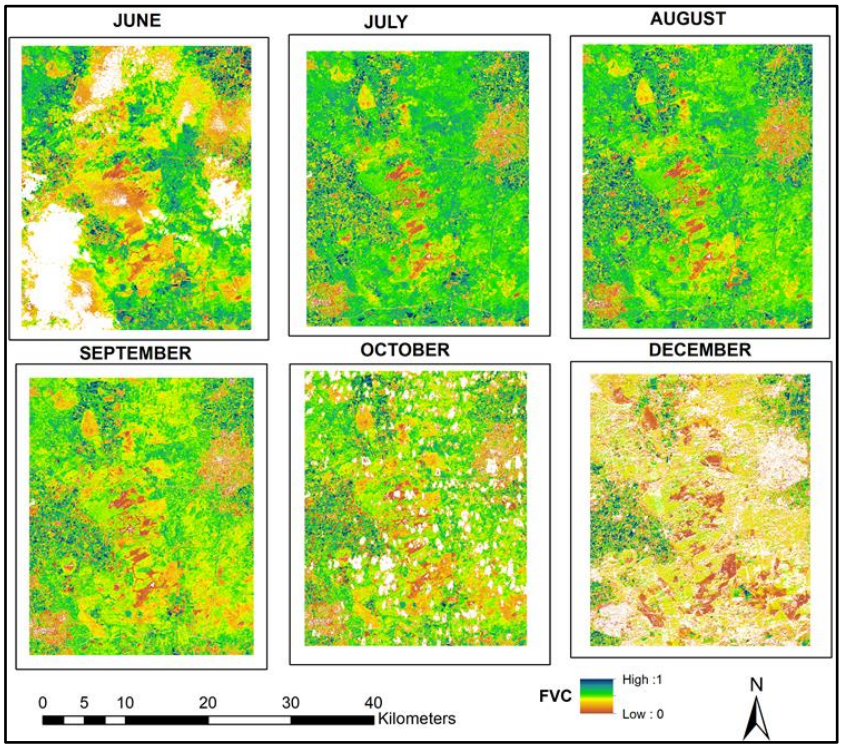

Figure 6-5: Spatial pattern of Fractional vegetation cover from June to December 2016

6.3. Canopy storage capacity

This present study, canopy storage capacity (Smax) of each land cover class was estimated from June to December 2016. The mean canopy storage capacity was estimated from LAI (Eq.1), and the mean Smax for each land cover class was obtained as 1.70, 1.94, 1.68, 0.97, and 0.78 mm for the broadleaf forest, coniferous forest, mixed forest, natural grassland, and pastures respectively.

6.4. Rainfall and Mean rainfall rate

Total rainfall (Pg) estimated within Six months from 01 June to December 2016 (excluding November, this month was not considered because during derivation of model parameters such as LAI and FVC the image of November was whole effected by clouds therefore it was removed from time series) was 347mm. The maximum gross rainfall was 117mm in June and a minimum of 20 mm in December (Figure 5-7). A total of 117 events were discriminated from hourly rainfall time series where all the rainfall events greater than 0.5mm/hr were only considered for estimation of interception loss. The mean rainfall rate per land cover class in whole season was estimated (Figure 6-6), there is high mean rainfall rate for all land cover classes in July and low mean rainfall rate in December. There is different rainfall intensities per land cover as was expected due to different locations of stations.

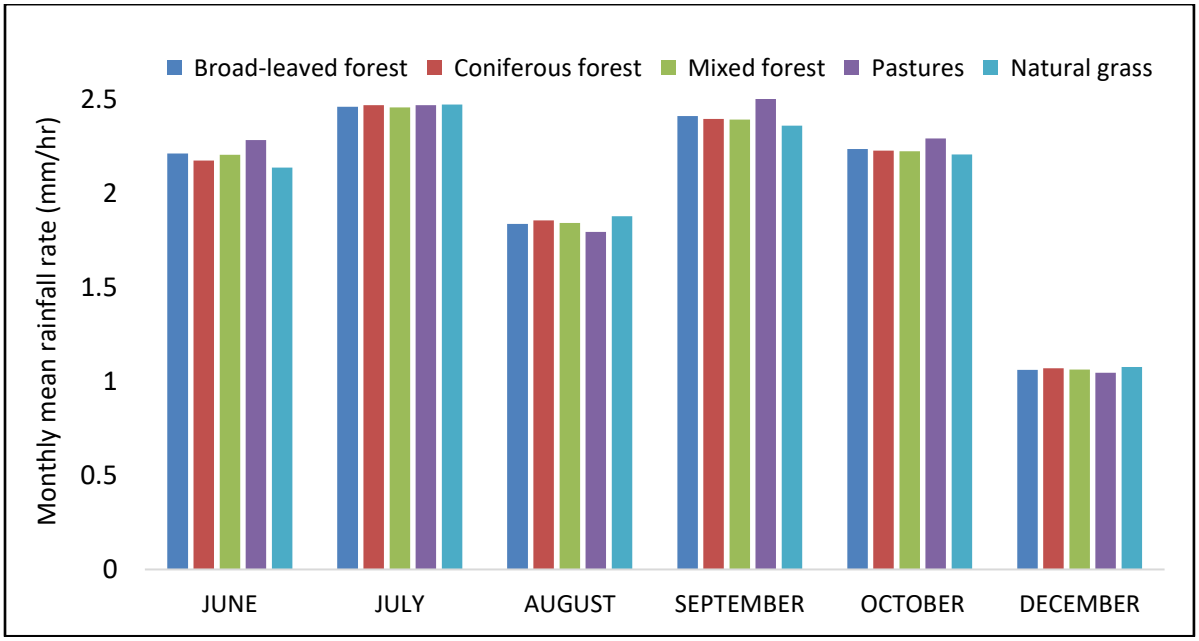

Figure 6-6: Mean hourly rainfall rate per month over the pixels for each land cover class from June to December 2016

6.5. Mean evaporation rate

The mean evaporation of the study area was calculated using Makkink reference evaporation equation. The mean evaporation of whole season (June to December 2016) with discontinuity of November ranges from 0 to 0.16mm/hr. The highest values are found in July and August and lowest values (approximately to zero) in December. The pastures have pixels with high values (0.16 mm/hr) in July followed by broadleaf forest, and natural grassland has the lowest values.

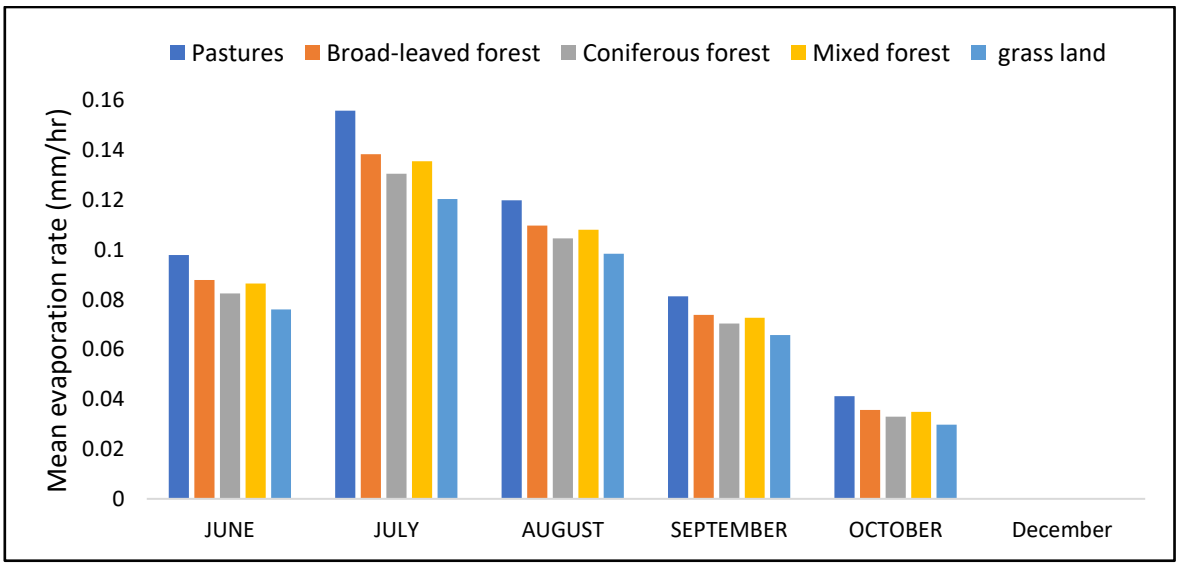

Figure 6-7: Temporal pattern of mean hourly evaporation rate per month for each land cover class from June to December 2016

6.6. Modelling rainfall interception

According to the previous studies for the case of the coniferous forest, the Gash, (1979) model was calibrated and validated by Cisneros et al. (2018) at the Speulderbos site using data-set from 19 June to October 2016. The overall interception loss measured was 39% of the gross rainfall (372mm) based on wet-canopy water balance. The LAI at that time was 4.5 m^2/m^2 measured using a LI-COR LAI 2000 plant Canopy analyzer. The same period (June to October 2016) was considered in this study to compare the results of measured and estimated interception using remote sensing.

Also, the monthly interception loss of five land cover classes was estimated from June to December 2016 with discontinuity of November as explained in methodology (Section5.3). The interception loss is calculated based on rainfall events ($Pg>$ 0.5 mm/hr) for each month.

Table 6-1: Monthly interception loss per landcover class from June to December 2016

Period	**Land cover classes**										
	BLF			**CF**		**MF**		**PS**		**NGL**	
	Rainfall (mm)	*I* (mm)	*% I*	*I* (mm)	*% I*	*I* (mm)	*% I*	*I* (mm)	*% I*	*I* (mm)	*% I*
JUN	117	36.40	31.16	32.54	27.86	34.29	29.36	21.83	18.68	22.97	19.66
JUL	67	25.59	38.03	23.98	35.62	23.80	35.36	17.02	25.3	15.90	23.62
AUG	64	22.22	34.47	20.92	32.45	20.59	31.94	15.08	23.4	12.52	19.41
SEP	27	10.71	39.72	9.62	35.65	9.81	36.37	7.68	28.5	5.51	20.42
OCT	52	10.11	19.48	9.39	18.1	9.55	18.41	6.01	11.6	4.04	7.78
DEC	20	1.77	9.02	3.37	17.17	2.66	14.00	2.98	15.20	1.22	6.24

The mean interception corresponding to each land cover class (broadleaf forest (BLF), coniferous forest (CF), mixed forest (MF), pastures (PS) and natural grassland (NGL)) in period of six months are 106.8mm, 99.82mm, 100.71mm, 70.6mm and 62.16mm represented with 28.7% , 27.8%, 27.6% , 20.4% , and 16.2% of gross rainfall respectively. The broad-leaved forest has high interception loss due to their maximum leaf area index, and fractional vegetation cover compare to other land cover classes. And low monthly values of interception are mostly found in December because during the winter period the most trees lose their leaves, which leads to a reduction of LAI and Smax as well. In general, pastures and grass have a low mean interception in the whole season.

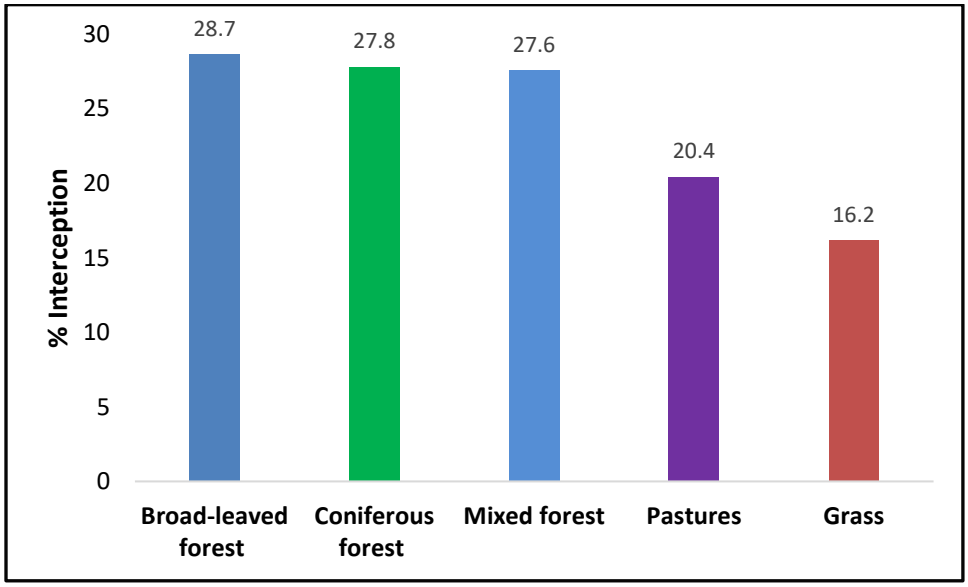

Figure 6-8: Mean interception loss per land cover from June to December 2016

6.7. The relationship between Leaf area index and interception loss

In order to quantify the relationship between leaf area index and the interception, the Coniferous land cover class was selected, and its LAI values (from 0 to 8m^2/m^2) and interception loss (from June to December 2016) were plotted on the graph, as LAI would be expected to change throughout with leaf life cycle,
Figure 6-9 shows the variation of interception with LAI. There is an offset of a low percentage of interception loss (1.8%) when LAI is zero due to the presence of branches.

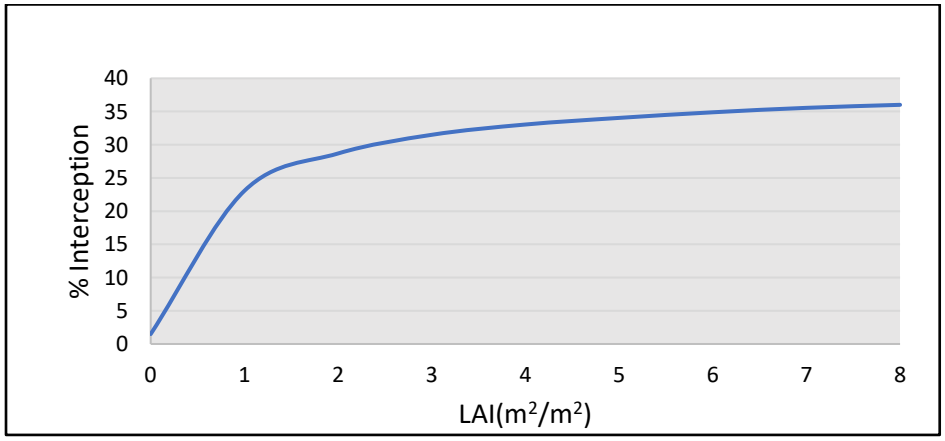

Figure 6-9: Variation of Interception with LAI for Coniferous from June to December 2016

Also, for the case of coniferous forest at speulderbos, part of the present study area, previous studies have indicated the relationship between leaf area index, canopy storage capacity and interception loss. For example, Bouten, Swart, & De Water, (1991) reported high interception loss due to high leaf area index resulting in high canopy storage capacity; this shows the strong relationship between the leaf area index and canopy storage capacity. As LAI increases the Smax increases rapidly as shown in Figure 6-10.

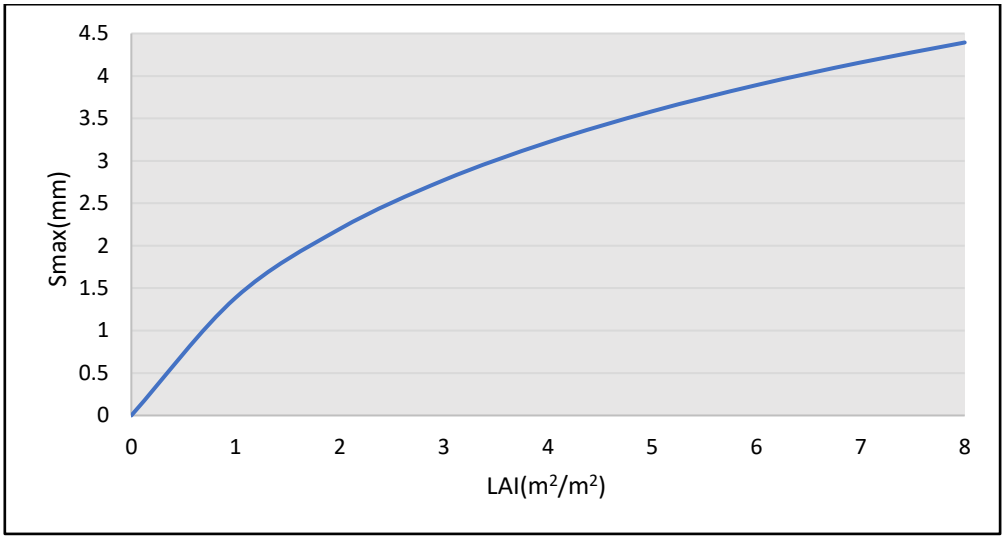

Figure 6-10: Relationship between leaf area index and canopy storage capacity

6.8. Sensitivity analysis of the model

There are five main parameters used in this model (RS-Gash model) include FVC, $\bar{R}$, $\overline{EV}$, LAI and $Smax$ To determine the reliability of the estimated rainfall interception loss, the sensitivity analysis was performed to every each of these parameters by changing the value of each while keeping others constant every month. To perform sensitivity of the model, the coniferous forest was randomly selected and, only the estimated values within five months (June, July, August, September, and October 2016) were taken in order to have continuous time series. Sensitivity analysis was performed to each of these five parameters per month, and the average interception loss was obtained (Figure 6-11).

The purpose of sensitivity analysis is to observe the behavior of the model to the variation of different input data values and also, to evaluate the overall model performance.
From the sensitivity analysis, the fractional vegetation cover (FVC) has a strong effect on the simulated interception loss (Figure 6-11a) compared to the other input parameters. As the fractional vegetational cover increases the simulated interception loss increases rapidly. This is because the FVC and LAI are dependent quantities (Carlson & Ripley, 1997) and interception loss depends on the leaf area and the capacity of water to retain the rainfall. Mean evaporation rate has also a big influence to simulated interception loss compared to other remaining parameters apart from FVC. In addition, the influence of mean rainfall rate to interception loss was also analysed where the scatter plot of different values of mean rain fall rate against the corresponding average interception loss was used (Figure 6-11c) the interception loss decreases exponentially as the mean rainfall rate increases.

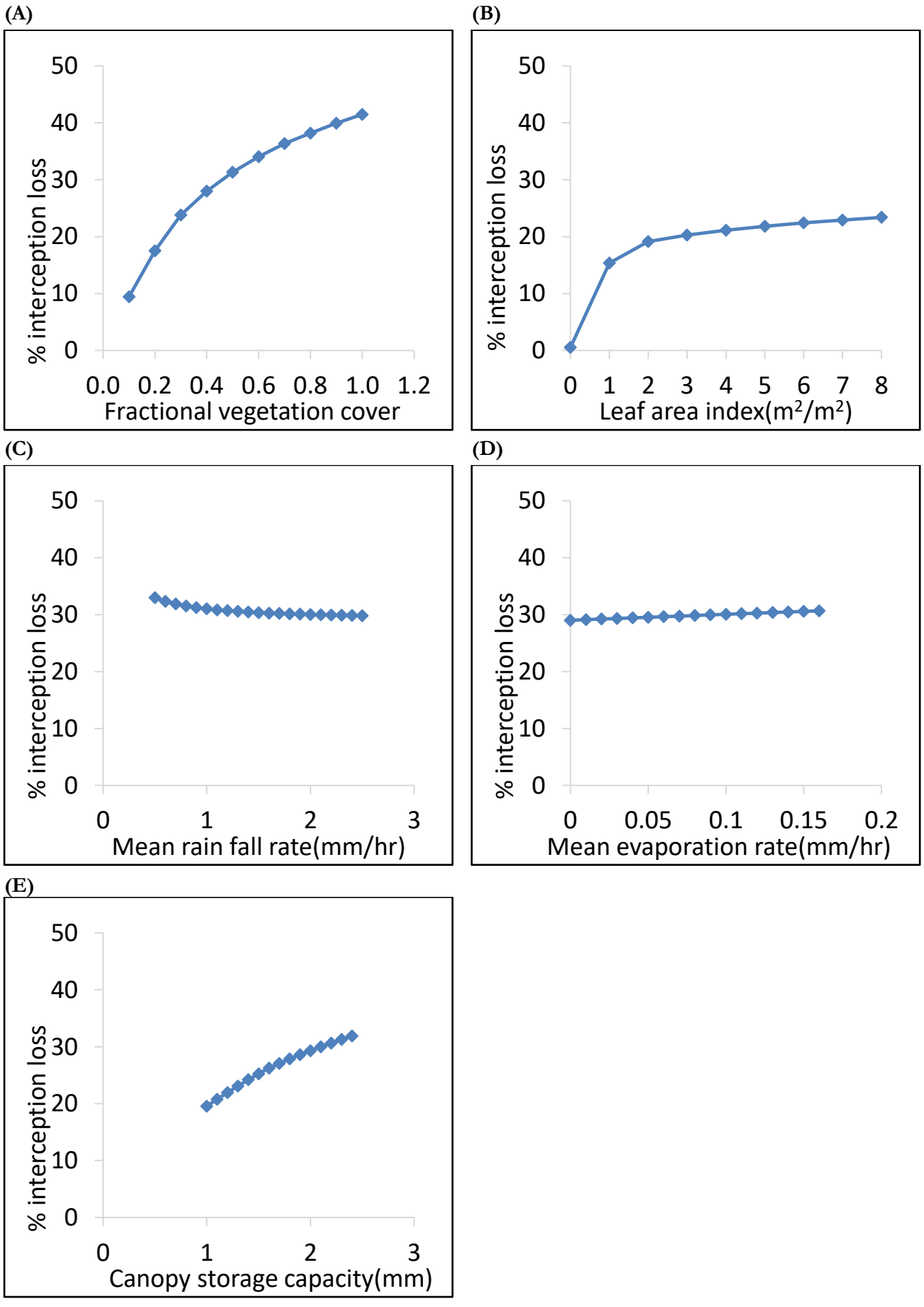

Figure 6-11: Sensitivity of estimated rainfall interception loss of coniferous forest on five parameters

6.9. Comparison between measured and estimated interception loss

In order to compare the measured interception loss from the previous study by Cisneros et al. (2018) and estimated interception loss of the present study, the Speulderbos site was chosen and coniferous plot was considered, only the estimated values within five months (June, July, August, September, and October 2016) were considered in order to match with the previous study period of field measurements. The Speulderbos site is part of the present study area (Veluwe area). This site offers a good opportunity to compare the estimated interception loss and measured interception loss for the case of Douglas-firm (coniferous forest), from the previous study by Cisneros et al. (2018) graduated PhD student in Department of Water Resources, ITC. The study was done from June to October 2016 and the following parameters were measured.

Table 6-2: Some of the parameters measured by Cisneros et al. (2018) at the coniferous plot

Parameters	Measured value
Leaf area index (LAI)	4.5 m^2/m^2
Canopy storage capacity($Smax$)	1.9 mm
Mean evaporation over mean rainfall rate ($\overline{EV}/\bar{R}$)	0.23 mm/hr
Mean evaporation rate ($\overline{EV}$)	0.2 mm/hr
Fractional vegetation cover (FVC)	1

And estimated values of the parameters for the coniferous forest in the present study are also presented in the table below. From the previous study by Cisneros et al. (2018) the measured LAI for the coniferous forest was 4.5m^2/m^2 and canopy storage capacity of 1.9mm. In the present study, the estimated mean LAI ranges from 1.6 to 2.2 m^2/m^2 and mean canopy storage capacity of 2.08 mm. The estimated parameter values of the present study area presented in Table 6-3 below, only the values estimated in five months (June to October 2016) were considered in order to match with the previous study period. From the previous study (coniferous plot), the measured interception loss was 39% of gross rainfall whereas in the present study the estimated interception loss is 30% of gross rainfall. The difference between the previous and present value is due to defense in fractional vegetation cover. Also, different models can produce different results.

Table 6-3: Monthly baseline estimated values for coniferous from June to October 2016

Period	Smax	LAI	FVC	$\bar{R}$	$\overline{EV}$
JUNE	1.94	1.64	0.44	2.18	0.08
JULY	2.33	2.21	0.54	2.47	0.13
AUGUST	2.19	1.98	0.50	2.16	0.41
SEPTEMBER	2.02	1.75	0.43	2.40	0.07
OCTOBER	1.93	1.62	0.36	2.23	0.03

7. DISCUSSIONS AND CONCLUSIONS

This study was carried out to quantify interception loss of different land cover classes on the large area using remote sensing observations from Sentinel-2 time series combined with RS-Gash model. First, the Leaf area index and Fractional vegetation cover monthly maps of the study area were derived from Sentinel-2 images within a period of Six months (June, July, August, September, October, and December) excluding November; this month the whole image was seriously affected by clouds. Different values of LAI and FVC of five different land cover classes; broadleaf forest (BLF), coniferous forest (CF), mixed forest (MF), pasture (PS) and natural grassland (NGL) were obtained per month and the values differ according to the period and land cover class (Appendix A.1 and AppendixA.2).

The land cover classes in the period of summer months tend to have larger LAI values compared to other months (Figure 6-1) shows the monthly LAI maps at 20m spatial resolution. These maps indicate significant temporal heterogeneities exist with LAI values varying from 0 to 8. The highest values of LAI are in months of early summer (June and July) for broad-leaved forests, coniferous forest, mixed forest and pastures except natural grassland has the lowest this indicates that the vegetation canopy was fully leafed, while the low values are found in December (winter season) during leaf abscission. And also, there are different pixel values (temporal variation) per land class in each month; this was expected due to the impact of clouds because during the cloud masking the affected pixels were removed which leads to the reduction of pixels in the images which had been affected by cloud cover. Therefore LAI is an important biophysical parameter that can be used to determine the temporal variation of vegetation at a certain area.

Fractional vegetation cover (FVC) maps of the study area were also derived (Figure 6-5) from June to December 2017; there are densely vegetated areas in July and August while less vegetated areas mostly appear in June and December due to the effect of clouds where some pixels were removed during the cloud removal. After FVC values per land cover class were obtained (Figure 6-4), there is temporal variation in pixel values across different land covers. The broadleaf forest covers high FVC of 67% which is high percent compared to other land cover classes due to their broad leaves. In general the high FVC values were found in July and August (summer season) where the most vegetation are at their peak production, and lowest values (10% to 30%) found in December (winter season) this is expected due to the fact that in this season the leaf abscission increases which leads to the reduction of canopy cover. Therefore, it is possible to estimate the spatial-temporal variation of LAI and FVC of different land cover classes at a larger area by remote sensing method.

The larger mean interception loss found is (28.65%) for broad-leaved forest and a low interception (16.19%) for natural grass. From the literature, normally different land cover types have different interception (Augusto, Ranger, Binkley, & Rothe, 2002), because of different vegetation structure, canopy properties and different leaf properties (Oerlemans & Vink, 2010). In the present study, there is also, temporal variability of interception loss across different land cover classes from June to December (Table 6-1). The high monthly interception losses are found in the early months of summer (June to September) and low values are found in December (winter season). This is because during the summer season the most vegetation are at their peak productivity and the have high leaf area index which increases the ability of vegetation to intercept more water, whereas in winter season most trees shade off their leaves.

The decrease in leaf amounts reduces leaf area index and vegetation canopy storage capacity as well. Therefore interception loss relies much on the ability of vegetation to hold water on its surface. Thus the magnitude of canopy storage capacity is dependent on the area of the leaf (Moors, 2012). This quantifies the relationship between the leaf area index and interception loss. Therefore, the change in leaf lifecycle has a strong influence on the estimation of interception loss. For instance, for the case of the coniferous forest, the previous studies of modelling such as canopy growth (Evers, Steingrover, & Jans, 1992), soil water dynamics (Tiktak & Bouten, 1994). It was pointed out that the high interception loss at the coniferous plot at that time was because of high leaf area index resulted in high canopy storage capacity as reported by Bouten, Swart, & De Water (1991) using microwave transmission.

Also, according to Bastiaanssen, Cheema, Immerzeel, Miltenburg, & Pelgrum (2012), there is a strong relationship between canopy storage capacity (Smax) and LAI. To accomplish this relationship the equation (Eq.1) developed by Vegas Galdos et al. (2012) was adopted in this study and the canopy storage capacity of each land cover was calculated from LAI (Table 5-2). And LAI as a biophysical parameter has a strong correlation with canopy interception (van Dijk & Bruijnzeel, 2001). Therefore, it was crucial to estimate canopy storage capacity (Smax) because of a lack of ground data. The present results suggest a good possibility of estimating Smax per land cover class from LAI (Eq.1). However, in this study, the f specific factor that depend on the type of landcover was obtained from the literature (Vegas Galdos et al., 2012), for future research this factor should be determined per land cover class. Thus, field data of Smax per land cover class remains necessary to reduce uncertainties in the estimation of interception loss.

Sensitivity analysis of RS-Gash model parameters; only one land cover class (coniferous forest) was selected and period of five months (June to October 2016) was also considered to have continuous time series of data. The sensitivity shows that the most sensitive parameter to the interception loss is fractional vegetation cover (FVC) because, as the fractional vegetational cover increases the simulated interception loss also, increases rapidly, so an increase in fractional vegetation cover increases the ability of vegetation to intercept more rainfall. For instance, during the dry period (summer) there is high interception loss, this implies in this study where there are high values of interception loss in months of summer compared to the other months (Table 6-1). Other results from sensitivity analysis are for Leaf area index and canopy storage capacity. According to Keim, Skaugset, & Weiler, (2006) leaf area index is the main predictor of canopy storage capacity, and LAI can provide the concrete base of comparing interception properties of different land cover classes (Aston, 1979). Therefore from the sensitivity analysis of LAI (Figure 6-11b), quantifies the relationship between leaf area index and interception loss.

Comparison between measured interception loss from the previous study by Cisneros et al. (2018) and the present study. For the case of coniferous forest the present results, the interception loss is 30% of gross rainfall based on the wet canopy (Pg>0.5mm/hr) and the previous results interception loss was 39% of gross rainfall. Normally Interception loss accounts between 20 and 40% in the coniferous forest (Le Maitre, Scott, & Colvin, 1999) . Therefore, the difference between the measured and estimated value of interception loss is because the previous study they used field measurement method which might be more accurate than remote sensing method has been used in the present study. Another reason could be the difference in fractional vegetation cover, from the previous study the fractional vegetation cover was one while in the present study the fractional vegetation cover ranges from 11% to 67%.

In addition, there are also other difference in canopy structures where from the previous study the measured leaf area index and canopy storage capacity were 4.5 m^2/m^2 and 1.9 mm respectively whereas in the present study estimated monthly mean leaf area index ranges from 1.6 in October to 2.2 m^2/m^2 in July (Table 6-3) and mean canopy storage capacity of 2.08 mm. Therefore, these changes in canopy structure can also contribute to the underestimation of interception loss of the present study.

In this study, Leaf area index and Fractional vegetation cover were derived from Sentinel-2 time series images. Earth observation data combined with RS-Gash model were used to quantify interception loss of different land cover classes on the large area. It is important to estimate interception as accurately as possible because rainfall interception by vegetation is an important hydrological process that can affect the spatial distribution of water input available for other processes such as evaporation and transpiration (Gómez, Giráldez, & Fereres, 2001). Different land cover classes have different interception loss (Figure 6-8) due to the fact that always forests have large interception loss than other land cover classes such as natural grassland and shrubs (Le Maitre et al., 1999).

In the present study, it is possible to estimate canopy storage capacity from Leaf area index.; however, the data were not enough, because some data like f factor that depend on the type of vegetation; it was a bit challenge to obtain the value of f factor for each land cover class, the values were obtained from literatures. Another challenge in this study was the low number of images due to the problem of cloud cover normally affect Sentinel-2 images, at least twenty four or twelve cloud free images were expected but only six images were obtained (Table 4-2). However, this limitation of images did not stop the progress of this research. The monthly interception loss of different land cover classes (broadleaf forest, coniferous forest, mixed forest, pasture and natural grassland) was successfully estimated (Table 6-1). The Sentinel-2 time series data can significantly contribute to the estimation of interception loss of different land cover classes on large scale and using these time series it is possible to assess temporal and spatial variation of LAI and FVC across different land cover classes.

8. RECOMMENDATIONS

- To reduce uncertainties in modelling interception loss and to improve quality of estimates, field measurements should be done at the whole study area for better comparison between measured and estimated interception loss by remote sensing observations.
- Future research, in cooperation with e.g. water Authorities, should include and improve on the land cover classification of the study area, and estimation of rainfall interception losses using the same approach. This would be beneficial to derive improved water balances needed by water authorities and in water management.
- Future research should also include the use of gap-filling techniques to obtain missing information in Sentinel-2 images. Sentinel-2 MSI data, have a wide field of view, high revisit time and spatial resolution, but because they present optical (VIS/IR) wavelength data, are highly affected by cloud cover, and these clouds were the main cause of missing information (in this study area). After successfully removing clouds and filling all the missing information, parameters like LAI, FVC and other biophysical parameters can be extracted from Sentinel-2 images, and complete time series generated.

LIST OF REFERENCES

Aston, A. R. (1979). Rainfall Interception by eight small Trees. *Journal of Hydrology*, *42*(3), 383–396. https://doi.org/10.1016/0022-1694(79)90057-X

Augusto, L., Ranger, J., Binkley, D., & Rothe, A. (2002). L. Augusto et al. Impact of several common Tree Species of European Temperate Forests on Soil fertility. *Annals of Forest Sciences*, *59*(3), 233–253. https://doi.org/10.1051/forest:2002020

Baillarin , Meygret , Petrucci , Lacherade , Tremas , Isola , Martimort, S. (2012). Sentinel-2 level 1 Products and Image processing performances. *International Geoscience and Remote Sensing Symposium (IGARSS)*, *39*, 7003–7006.

Bakar, A. A. A., Bin Baki, A., Bt Hamzah, N., Bin Yusop, Z., & Bin Khalil, M. K. (2012). Throughfall, Stemflow and Interception Loss of Artificial Tropical Forest. *IEEE Colloquium on Humanities, Science and Engineering Research*, *3–4*, 98–102. https://doi.org/10.1109/CHUSER.2012.6504289

Bastiaanssen, W. G. M., Cheema, M. J. M., Immerzeel, W. W., Miltenburg, I. J., & Pelgrum, H. (2012). Surface Energy Balance and Actual Evapotranspiration of the Transboundary Indus Basin estimated from Satellite measurements and the Etlook Model. *Water Resources Research*, *48*(11), 1–16. https://doi.org/10.1029/2011WR010482

Bouten, W., Swart, P. J. F., & De Water, E. (1991). *Microwave Transmission, Anew Tool in Forest Hydrological Research*. *Journal of Hydrology* (Vol. 124). https://doi.org/0022-1694

Calder. (1998). *Water use by Forest, Limits and Controls (Report No: 18)*. Retrieved from http://www.heronpublishing.com

Calder, I., Hofer, T., Vermont, S., & Warren, P. (2007). Towards a New understanding of Forests and Water. *Unasylva*, *58*(229), 3–10. https://doi.org/10.1057/9781137034328

Carlson, T. N., & Ripley, D. A. (1997). On the Relation between NDVI, Fractional Vegetation Cover, and Leaf Area Index. *Remote Sensing of Environment*, *62*, 241–252. https://doi.org/10.1016/S0034-4257(97)00104-1

Chen, Y. Y., & Li, M. H. (2016). Quantifying Rainfall Interception Loss of a Subtropical Broadleaved Forest in central Taiwan. *Water (Switzerland)*, *8*, 1–19. https://doi.org/10.3390/w8010014

Cisneros, Tol, V., & Ghimire. (2018). The influence of Long-term changes in Canopy Structure on Rainfall Interception Loss : a case study in Speulderbos , the Netherlands. *European Geosciences Union*, *22*, 3701–3719. Retrieved from https://doi.org/10.5194/hess-22-3701-2018

Coluzzi, R., Imbrenda, V., Lanfredi, M., & Simoniello, T. (2018). A first Assessment of the Sentinel-2 Level 1-C Cloud mask Product to support Informed Surface analyses. *Remote Sensing of Environment*, *217*, 426–443. https://doi.org/10.1016/j.rse.2018.08.009

Cosandey, C., Martin, C., Savina, L., Cosandey, C., Martin, C., Savina, L., & The, J. D. (2003). The Impact of Interception Losses on the Water balance in Forested Mountains range. *Journal of Hydrology*, *67*, 79–84.

Crockford, R. H., & Richardson, D. P. (2000). Partitioning of Rainfall into Throughfall, Stemflow and Interception: Effect of Forest type, Ground Cover and Climate. *Hydrological Processes*, *14*, 2903–2920. https://doi.org/10.1002/1099-1085

Cui, Y., & Jia, L. (2014). A modified Gash model for estimating Rainfall Interception Loss of Forest using Remote Sensing Observations at Regional Scale. *Water (Switzerland)*, *6*, 993–1012. https://doi.org/10.3390/w6040993

Cui, Y., Zhao, P., Yan, B., Xie, H., Yu, P., Wan, W., … Hong, Y. (2017). Developing the Remote sensing-Gash Analytical Model for estimating Vegetation Rainfall Interception at very High Resolution: A case study in the Heihe River Basin. *Journal of Remote Sensing*, *9*(661), 1–12. https://doi.org/10.3390/rs9070661

De Jong, S. M., & Jetten, V. G. (2007). Estimating Spatial Patterns of Rainfall Interception from Remotely Sensed Vegetation Indices and Spectral Mixture Analysis. *International Journal of Geographical Information Science*, *21*, 529–545. https://doi.org/10.1080/13658810601064884

Dijkshoorn, M. (2017). The Vegetation Development and Drift-sand Dynamics in the Kootwijkerveen , the Netherlands : the role of Human Impact and Climate Variability (M.Sc.Thesis).

Ekhuemelo, D. O. (2016). Importance of Forest and Trees in Sustaining Water Supply and Rainfall. *Research Gate*, *8*, 273–280. Retrieved from https://www.researchgate.net/publication

ESA. (2012). ESA's Optical High-Resolution Mission for GMES Operational Services.

ESA. (2015). *Sentinel-2 User Handbook*. *Sentinel-2 User Handbook*. Noordwijk, The Netherlands: ESA, European Commission. https://doi.org/GMES-S1OP-EOPG-TN-13-0001

European Environment Agency. (2012). Corine Land Cover. Retrieved December 7, 2018, from https://land.copernicus.eu/pan-european/corine-land-cover/clc-2012

Evers, P. W., Steingrover, E. G., & Jans, W. W. P. (1992). Ecophysiological Relations in Two Douglas fir Stands in the Netherlands. *Acta Botanica Neerlandica*, *41*(1), 89–101. https://doi.org/10.1111/j.1438-8677.1992.tb01313.x

Gash, Lloyd, L. (1995). *Estimating Sparse Forest Rainfall Interception with An analytical Model*. *Journal of Hydrology* (Vol. 170). Retrieved from https://ac.els-cdn.com/002216949502697

Gash, J. H. C. (1979). An analytical Model of Rainfall Interception by Forests. *Quarterly Journal of the Royal Meteorological Society*, *105*, 43–55. https://doi.org/10.1002/qj.49710544304

Gómez, J. A., Giráldez, J. V., & Fereres, E. (2001). Rainfall Interception by Olive Trees in Relation to Leaf Area. *Agricultural Water Management*, *49*, 65–76. https://doi.org/10.1016/S0378-3774(00)00116-5

Hein, L. (2011). Economic Benefits Generated by Protected Areas: the Case of the Hoge Veluwe Forest, the Netherlands. *Ecology and Society*, *16*(2), 1–13. Retrieved from http://www.ecologyandsociety.org/vol16

Hiemstra, P., & Sluiter, R. (2011). *Interpolation of Makkink Evaporation in the Netherlands*. *De Bilt, 2011 | Technical report; TR-327*. The Hague: Royal Netherlands Meteorological Institute, Ministry of Infrastructure and the Environment. Retrieved from http://www.numbertheory.nl/files/report_evap.pdf

Horton, R. (1919). Rainfall Interception: Monthly Weather Review. *Journal of Hydrology*, *47*(9), 603–623.

Jaffrain, G. (2017). Corine Landcover 2012 Final Validation Report. *Copernicus Land Monitoring*, 214. Retrieved from https://land.copernicus.eu/user-corner/technical-library/clc-2012-validation-report-1

Keim, R. F., Skaugset, A. E., & Weiler, M. (2006). Storage of Water on Vegetation under Simulated Rainfall of varying Intensity. *Advances in Water Resources*, *29*, 974–986. https://doi.org/10.1016/j.advwatres.2005.07.017

Klaasen, W., Bosveld, F., & de Water, E. (1995). Water Storage and Evoporation as Constituents of Rainfall Interception. *Journal of Hydrology*, *212–213*, 36–50. https://doi.org/10.1016/S0022-1694(98)00200-5

Klaassen, Bosveld, F. ;, & de Water, E. (1998). Water Storage and Evaporation as Constituents of Rainfall Interception. *Journal of Hydrology*, *212–213*, 36–50. https://doi.org/10.1016/S0022-1694(98)00200-5

Le Maitre, D. C. Le, Scott, D. F., & Colvin, C. (1999). A review of Information on Interactions between Vegetation and Groundwater. *Water Research*, *25*(2), 137–152. Retrieved from http://www.wrc.org.za

Mandanici, E., & Bitelli, G. (2016). Preliminary Comparison of Sentinel-2 and Landsat 8 Imagery for a Combined Use. *Journal of Remote Sensing*, *8*, 10. https://doi.org/10.3390/rs8121014

Massman, W. J. (1983). The Derivation and Validation of a New Model for the Interception of Rainfall by Forests. *Agricultural Meteorology*, *28*, 261–286. Retrieved from https://doi.org/10.1016/0002-1571(83)90031-6

Miralles, D. G., Gash, J. H., Holmes, T. R. H., De Jeu, R. A. M., & Dolman, A. J. (2010). Global canopy interception from satellite observations. *Journal of Geophysical Research Atmospheres*, *115*(D16122), 1–8. https://doi.org/10.1029/2009JD013530

Mo, X., Liu, S., Lin, Z., & Zhao, W. (2004). Simulating Temporal and Spatial Variation of Evapotranspiration over the Lushi basin. *Journal of Hydrology*, *285*, 125–142. https://doi.org/10.1016/j.jhydrol.2003.08.013

Moors, E. (2012). Water Use of Forests in the Netherlands. *De Vrije Universiteit Amsterdam,* 291.

Muzylo, A., Llorens, P., Valente, F., Keizer, J. J., Domingo, F., & Gash, J. H. C. (2009). A review of Rainfall Interception Modelling. *Journal of Hydrology*, *370*, 191–206. https://doi.org/10.1016/j.jhydrol.2009.02.058

Oerlemans, R. R. R., & Vink, R. P. (2010). *Rainfall Interception Experiments and Interception Mapping using Remote Sensing (M. Sc.Thesis)*. Faculty of Geosciences, Utrecht University, Utrecht. Retrieved from http://igitur-archive.library.uu.nl/student-thesis/2010-1215-200302/Thesis - Final Version.pdf

Rutter, A. J., Kershaw, K. A., Robins, P. C., & Morton, A. J. (1971). A predictive Model of Rainfall Interception in Forests. *AgriculturalMeteorology*, *9*, 367–384. Retrieved from https://www.sciencedirect.com/science/article/pii/0002157171900343

Rutter, A. J., Morton, A. J., & Robins, P. C. (1975). A Predictive Model of Rainfall Interception in Forests. II. Generalization of the Model and Comparison with Observations in Some Coniferous and Hardwood Stands. *Journal of Applied Ecology*, *12*(1), 367–380. https://doi.org/10.2307/2401739

Song, W., Mu, X., Ruan, G., Gao, Z., Li, L., & Yan, G. (2017). Estimating Fractional Vegetation Cover and the Vegetation Index of Bare Soil and Highly Dense Vegetation with Physically based Method. *International Journal of Applied Earth Observation and Geoinformation*, *58*, 168–176. https://doi.org/10.1016/j.jag.2017.01.015

Tiktak, A., & Bouten, W. (1994). Soil Water Dynamics and Long-term Water balances of a Douglas fir Stand in the Netherlands. *Journal of Hydrology*, *156*, 265–283. https://doi.org/10.1016/0022-1694(94)90081-7

van Dijk, A. I. J. ., & Bruijnzeel, L. . (2001). Modelling Rainfall Interception by Vegetation of Variable Density using an adapted Analytical Model. Part 1. Model Description. *Journal of Hydrology*, *247*, 230–238. https://doi.org/10.1016/S0022-1694(01)00392-4

Vegas Galdos, F., Álvarez, C., García, A., & Revilla, J. A. (2012). Estimated distributed Rainfall Interception using a Simple Conceptual Model and Moderate Resolution Imaging Spectroradiometer (MODIS). *Journal of Hydrology*, *468–469*, 213–228. https://doi.org/10.1016/j.jhydrol.2012.08.043

APPENDICES

Appendix A.1: Monthly statistical Leaf area index values per land cover class of the study area

Table 8-1: LAI per land cover class in June

Land cover class	Number of pixels	Min	Max	Mean	STD
Pastures	162468	0	8	1.8	1.4
Broad-leaved forest	64923	0	8	2.2	1.0
Coniferous forest	573485	0	8	1.6	0.7
Mixed forest	382535	0	8	2.1	0.8
Natural grass land	9427	0	6	2	0.9

Table 8-2: LAI per land cover class in July

Land cover class	Number of pixels	Min	Max	Mean	STD
Pastures	196552	0	8	2.2	1.3
Broad-leaved forest	68972	0.2	6	2.7	0.5
Coniferous forest	700691	0	8	2.2	0.6
Mixed forest	426740	0	8	2.5	0.6
Natural grass land	10496	0	6.2	2	0.8

Table 8-3: LAI per land cover class in August

Land cover class	Number of pixels	Min	Max	Mean	STD
Pastures	196839	0	8	2	1.1
Broad-leaved forest	68967	0	5.2	2.4	0.5
Coniferous forest	700853	0	8	2	0.5
Mixed forest	426800	0	7	2.2	0.5
Natural grass land	10497	0	5	1.6	0.7

Table 8-4: LAI per land cover class in September

Land cover class	Number of pixels	Min	Max	Mean	STD
Pastures	196043	0	8	1.6	0.9
Broad-leaved forest	68948	0	5.7	2.1	0.5
Coniferous forest	699586	0	6.7	1.7	0.5
Mixed forest	425947	0	6.6	2	0.6
Natural grass land	10473	0	3.9	1.1	0.7

Table 8-5: LAI per land cover class in October

Land cover class	Number of pixels	Min	Max	Mean	STD
Pastures	182910	0	8	1.5	0.9
Broad-leaved forest	61290	0	7.2	1.9	0.7
Coniferous forest	600328	0	8	1.6	0.6
Mixed forest	381446	0	7.5	1.8	0.6
Natural grass land	8445	0	3.9	1	0.6

Table 8-6: LAI per land cover class in December

Land cover class	Number of pixels	Min	Max	Mean	STD
Pastures	173791	0	5.7	0.9	0.6
Broad-leaved forest	27700	0	2.5	0.5	0.4
Coniferous forest	436805	0	3.3	0.8	0.3
Mixed forest	222974	0	3.2	0.8	0.4
Natural grass land	7692	0	2.5	0.4	0.3

Appendix A.2: Monthly statistical Fractional vegetation cover values per land cover class of the study area

Table 8-7 : FVC values per land cover class in June

Land cover class	Number of pixels	Min	Max	Mean	STD
Pastures	162468	0	1	0.5	0.3
Broad-leaved forest	64923	0	1	0.6	0.2
Coniferous forest	573485	0	1	0.5	0.1
Mixed forest	382535	0	1	0.6	0.2
Natural grass land	9427	0	1	0.6	0.2

Table 8-8: FVC values per land cover class in July

Land cover class	Number of pixels	Min	Max	Mean	STD
Pastures	196552	0	1	0.6	0.2
Broad-leaved forest	68972	0	1	0.7	0.1
Coniferous forest	700691	0	1	0.5	0.1
Mixed forest	426740	0	1	0.6	0.1
Natural grass land	10496	0	1	0.6	0.2

Table 8-9: FVC value per landcover class in August

Land cover class	Number of pixels	Min	Max	Mean	STD
Pastures	196839	0	1	0.6	0.2
Broad-leaved forest	68967	0	1	0.6	0.1
Coniferous forest	700853	0	1	0.5	0.1
Mixed forest	426800	0	1	0.6	0.1
Natural grass land	10497	0	1	0.5	0.1

Table 8-10: FVC values per land cover class in September

Land cover class	Number of pixels	Min	Max	Mean	STD
Pastures	196043	0	1	0.5	0.2
Broad-leaved forest	68948	0	1	0.5	0.1
Coniferous forest	699586	0	1	0.4	0.1
Mixed forest	425947	0	1	0.5	0.1
Natural grass land	10473	0	1	0.4	0.2

Table 8-11 : FVC values per land cover class in October

Land cover class	Number of pixels	Min	Max	Mean	STD
Pastures	182910	0	1	0.5	0.2
Broad-leaved forest	61290	0	1	0.5	0.2
Coniferous forest	600328	0	1	0.4	0.1
Mixed forest	381446	0	1	0.5	0.1
Natural grass land	8445	0	1	0.3	0.1

Table 8-12: FVC values per land cover class in December

Land cover class	Number of pixels	Min	Max	Mean	STD
Pastures	173791	0	1	0.3	0.2
Broad-leaved forest	27700	0	0.6	0.2	0.1
Coniferous forest	436805	0	0.8	0.2	0.1
Mixed forest	222974	0	0.8	0.2	0.1
Natural grass land	7692	0	0.7	0.2	0.1